JNC TN8400 2001-016

Modeling Studies of Saline Type Groundwater Evolution

— A Test Case for the Mobara Groundwater Chemistry, Japan —

February 2001

TOKAI WORKS
JAPAN NUCLEAR CYCLE
DEVELOPMENT INSTITUTE

〒319-1184　茨城県那珂郡東海村大字村松4番地49
核燃料サイクル開発機構
技術展開部　技術協力課

Inquiries about copyright and reproduction should be addressed to:
Technical Cooperation Section,
Technology Management Division,
Japan Nuclear Cycle Development Institute
4-49 Muramatsu, Tokai-mura, Naka-gun, Ibaraki 319-1184,
Japan

◎

Modeling Studies of Saline Type Groundwater Evolution - A Test Case for the Mobara Groundwater Chemistry, Japan -

Hiroshi Sasamoto[1)], Mikazu Yui[1)], Randolph C Arthur[2)]

Abstract

Mobara area is located in "dissolved-in-water" type natural gas region that is called as *"South Kanto gas field"*. In the Mobara area, investigation of volcanic glass buried in a marine based argillaceous rock has been carried out as natural analogue study in order to infer the long-term durability of waste glass in compacted bentonite. Modeling studies of saline type groundwater evolution has been performed using the saline type groundwater data derived from natural analogue study at the Mobara area. The results of this study are summarized below.

- The Mobara groundwaters are sampled from deep boreholes, so the water pressure of Mobara groundwater should be high. And the Mobara groundwaters contain high concentrations of dissolved gases. Therefore, it is needed to check whether the groundwater sampled at surface keep the *in-situ* groundwater conditions.
- As an example, pH value for the *in-situ* Mobara groundwater is estimated by $CO_2(g)$ *back-titration modeling*, which causes the separated gas at surface to dissolve in the groundwater. The result shows that the estimated pH value for the *in-situ* groundwater is 1 unit (in maximum) lower than the measured pH value at the surface. In the $CO_2(g)$ *back-titration modeling*, it is assumed that the *in-situ* groundwater should be equilibrated with calcite, considering the observed mineralogy of the formation.

The estimation method described above seems to be sound through the discussions with international experts. The following issues may be needed to estimate more realistic *in-situ* groundwater chemistry.

- possibility of concurrent degassing and precipitation of carbonate minerals, and
- effects on groundwater redox conditions by other gases, such as $H_2S(g)$, though present in trace amounts.

---

1) Barrier Performance Group., Waste Isolation Research Division, Waste Management and Fuel Cycle Research Center, Tokai Works, JNC

2) Monitor Scientific, L.L.C., Denver, Colorado USA

海水系地下水の水質変遷に関するモデリング
－茂原地下水を一例とした研究－

笹本 広[1)]，油井 三和[1)]，Randolph C Arthur[2)]

要 旨

茂原地域は，南関東ガス田と呼ばれる水溶性天然ガス鉱床地域に位置する。茂原地域では，圧縮ベントナイト中の廃棄物ガラスの長期耐久性評価に資するため，海成泥質岩中に含まれる火山ガラスの調査が行われている。この調査の際に得られた海水系地下水の水質データを基に海水系地下水の水質変遷に関するモデリングを行った。以下に，その結果をまとめる。

・茂原地域の地下水は，採水深度が深いため水圧が高く，多量の溶存ガスを含む。そのため，地表で採取された地下水は，原位置の状態を反映しているかどうかチェックする必要がある。
・一例として，地表で脱ガスした炭酸ガスを地下水に溶存させる方法により，茂原地域における原位置での地下水のpHを推定した。その結果，地表でのpH測定値に比べて，最大1程度，pHが低くなることが推定された。推定にあたっては，地層中に認められる鉱物組成を考慮し，地下水が方解石に対して飽和であると仮定した。

上記の様な推定方法は，海外の専門家との議論においても妥当であると考えられた。また，以下の様な検討を行うことにより，原位置の状態をより現実的に推定できる可能性が示唆された。

・炭酸ガスの脱ガスと同時に，炭酸塩鉱物の沈殿反応の可能性
・炭酸ガス以外の溶存ガス（例えば，硫化水素ガス）による酸化還元状態への影響

1) 東海事業所 環境保全・研究開発センター 処分研究部 処分バリア性能研究グループ
2) Monitor Scientific, L.L.C., Denver, Colorado USA

Table of Contents

List of Tables

List of Figures

List of Appendices

1. BACKGROUND

Candidate sites for the geological disposal of high-level nuclear wastes (HLW) in Japan have not yet been selected. Such sites will, however, consist of a crystalline or sedimentary host rock into which the HLW will be emplaced at depths of several hundred meters. The host rock will function as a natural barrier to the migration of radioactive elements from the waste to the biosphere.

The Japan Nuclear Cycle Development Institute (*JNC*[1]) has carried out field studies to characterize the hydrogeological and geochemical properties of several types of geologic systems in Japan: granodioritic host rocks (Kamaishi area), granitic host rock and overlying Tertiary sediments (Tono area), Pliocene-aged mudstones and sandstones (Horonobe area), and intercalated mudstones and volcaniclastic sediments (Mobara area; which is not *in-situ* tests site like the others noted above, but rather an area that has been investigated as a natural analogue of engineered barrier materials).

The objectives of the field studies include *characterization* of actual subsurface geochemical conditions in potential repository host rocks, and *testing* of equilibrium-based geochemical models of groundwater chemistry and evolution in relation to the actual behavior of real groundwater systems. Such *testing* of geochemical models of groundwater evolution is necessary to strengthen the underlying concepts incorporated in the groundwater evolution model used in the H-12 performance assessment.

Sasamoto *et al.* (1999a,b) describe geochemical models appropriate for conditions at the Kamaishi and Tono *in-situ* tests sites, respectively. The groundwaters at Kamaishi and Tono are fresh, but those at Mobara are saline. The results of geochemical modeling of selected aspects of the groundwater chemistry at the Mobara site are presented in this report (Section 2). A discussion of the results is summarized in Section 3.

[1] JNC was established in 1998, and is responsible for many of the R&D functions supporting nuclear waste management that were formerly assigned to the Power Reactor and Nuclear Fuel Development Corporation (PNC).

2. GEOCHEMICAL MODELS OF GROUNDWATER EVOLUTION

2.1 Introduction

Four types of hypothetical groundwaters were considered in the H-3 performance assessment. Their characteristics were defined by considering the origin and evolution of groundwaters in various types of geological environments found commonly throughout Japan (PNC, 1992). It was assumed that the flow rate of deep groundwaters is generally slow, and thus that water-rock interactions occur over long periods of time. The duration of water-rock interactions was further assumed to be sufficiently long that equilibrium constraints would control groundwater chemistry. This general approach was also used to define the characteristics of hypothetical groundwaters considered in the H-12 performance assessment (Yui *et al.*, 1999).

Groundwaters were sampled by JNC in the Mobara area as part of a natural analogue study designed to gain insights into the long-term behavior of nuclear-waste glasses in contact with bentonite buffer materials. The results of this study, including a discussion of the general geological conditions, groundwater chemistry and mineralogy of the argillaceous sedimentary rocks of the Mobara area, are described by Kamei *et al.* (2000). The Mobara area includes the well-known *"South Kanto gas field"* (Natori, 1997). Sugisaki *et al.* (1962) describe the compositions of groundwaters and gases sampled from this field. Mobara groundwaters are saline, and are typical of saline type groundwaters associated with oil, gas and coal fields represented in JNC's extensive database of groundwater samples from throughout Japan (Yui *et al.*, 1999).

Interpretations of geochemical controls on the compositions of Mobara groundwater are complicated by the high concentrations of dissolved gases and the relatively high hydrostatic pressures at depths from which the available samples were obtained. The present study focuses primarily on characterizing the *in-situ* subsurface geochemical conditions at the Mobara site, based on site-characterization results reported by Kamei *et al.* (2000) and Sugisaki *et al.* (1962). In contrast, the Kamaishi and Tono studies deal with both the characterization of subsurface geochemical conditions at these sites as well as testing of equilibrium-based geochemical models appropriate for these sites.

2.2 Geological Setting

2.2.1 Locality and Geological Features

The Mobara area is located approximately 50 km southeast of Tokyo (Figure 1). Neogene sedimentary rocks of the Kazusa group represent the geology of this area. Formations within the Kazusa group are identified in Figure 2. Of primary interest to the present study is the Otadai formation, which formed about 1 Ma (Watanabe and Danhara, 1996). It consists of clay-rich rocks whose physical properties (*e.g.*, dry-density, porosity, hydraulic conductivity) are similar to bentonite, which is planned for use as an engineered buffer material in Japan's HLW repository. This formation also includes volcaniclastic sediments composed of scoria or volcanic ash, whose chemical properties (*e.g.*, SiO_2 content) are similar to HLW glass. The Otadai formation was therefore selected as a potential natural analogue of the long-term behavior of HLW glass in contact with bentonite buffer materials (Kamei *et al.*, 2000). A schematic cross section of the Otadai formation is shown in Figure 3, where the location of a scoriaceous tuff member is indicated, as is the location where a sample of this member was obtained for use in the natural analogue study.

A number of gas-producing wells intersect the Kazusa group (Figure 3). Groundwaters and gases produced from these wells have been sampled. Typical compositions of gases separated at the wellhead are as follows (Natori, 1997):

- $CH_4(g) = 98\%$
- $CO_2(g) = 1.8\%$, and
- $N_2(g)+Ar(g)+H_2(g) = 0.2\%$.

2.2.2 Groundwater Chemistry

The chemical and isotopic compositions of groundwaters and surface waters from the Mobara reported by Kamei *et al.* (2000) are shown in Table 1. Other analyses reported by Sugisaki *et al.* (1962) of groundwaters and gases from the South Kanto gas field are shown in Tables 2 and 3, respectively.

The locations of gas wells from which these groundwater and gas samples were obtained are shown in Figure 4. The rate of groundwater flow through these wells is several hundred m^3 per day, and is controlled by artesian conditions. The wells were drilled several decades ago,

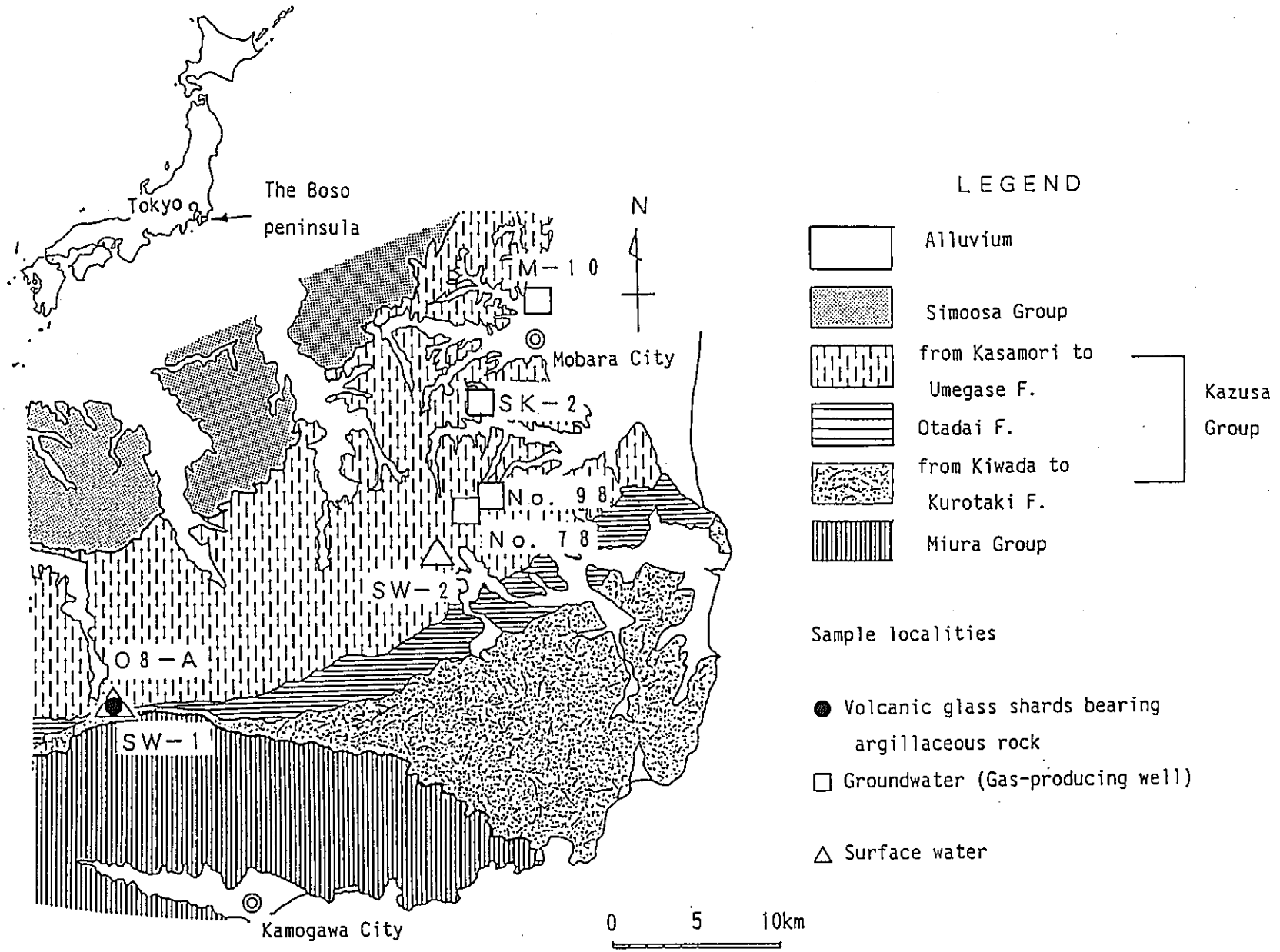

***Figure 1**: Geological map of the Boso peninsula showing groundwater sampling points (from Kamei et al., 2000)*

***Figure 2**: Stratigraphy of the east-central part of the Boso peninsula (from Kamei et al., 2000)*

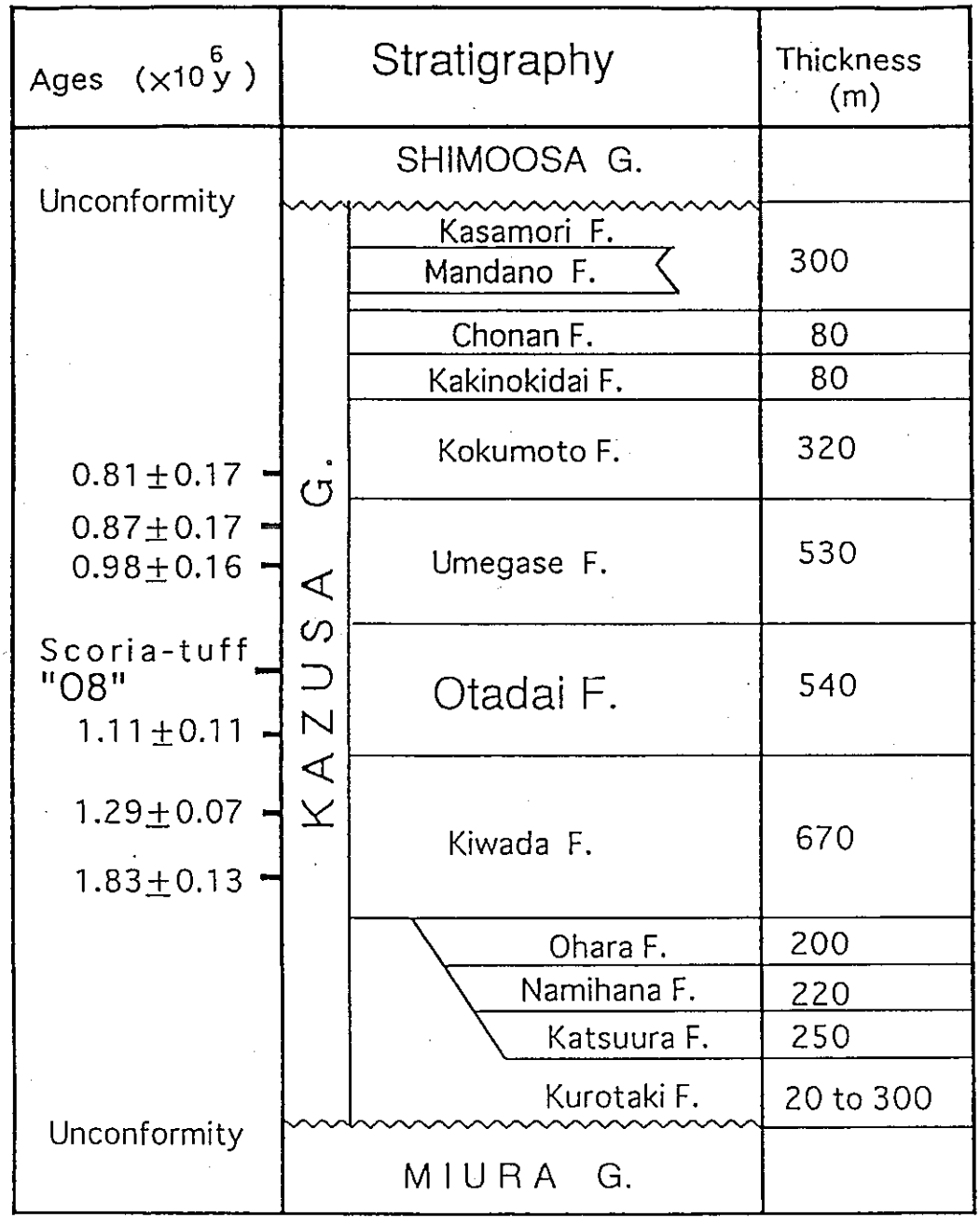

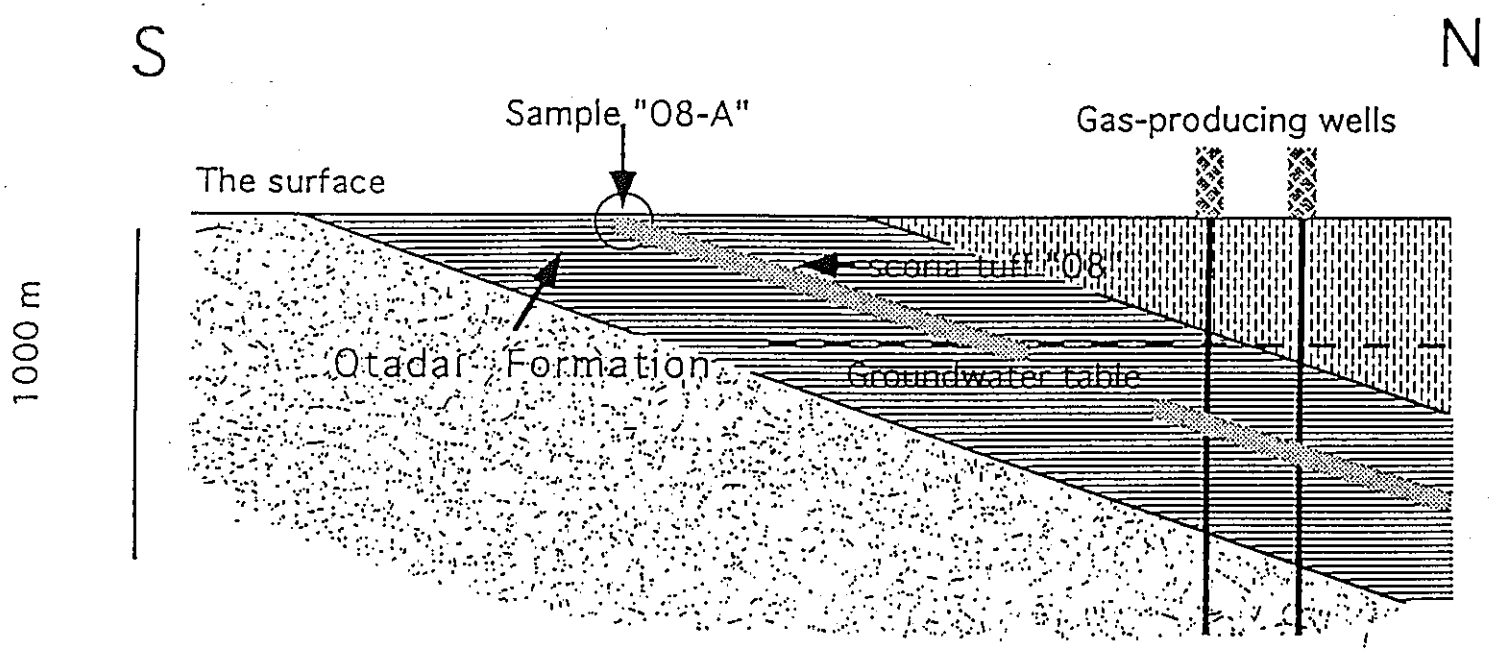

***Figure 3**: Conceptual geological cross section of the Mobara area (from Kamei et al., 2000)*

Table 1 : Chemistry of groundwaters from the Mobara area (data from Kamei et al., 2000)

	Unit	Mobara Area Ground Water Data								Mobara Area Surface Water Data			
Sample No.		No.78		No.98		SK-2		M-10		SW-1		SW-2	
Strainer depth	m	960-1202		895-1301		717-1140		517-949		-		-	
Water temp	℃	27.8		28.6		24		24.9		14.7		14.6	
Electric conductivity	mS/m	4770		4290		3640		4660		250		130	
pH		7.86		7.79		7.94		7.74		7.9		7.7	
Eh (vs.SHE)	mV	-50		-34		-73		-52		427		422	
		mg/l	meq/l	mg/l	meq/l	mg/l	meq/l	mg/l	meq/l	mg/l	meq/l	mg/l	meq/l
Na	-	10700	465.42	10400	452.37	7410	322.31	9390	408.44	22.40	0.97	6.27	0.27
K	-	3020	77.24	2960	75.70	2120	54.22	2760	70.59	2.91	0.07	1.10	0.03
Ca	-	229	11.43	219	10.93	145	7.24	174	8.68	23.20	1.16	15.20	0.76
Mg	-	315	25.90	339	27.88	223	18.34	362	29.77	4.80	0.39	2.55	0.21
Fe++	-	0.98	0.04	2.25	0.08	0.86	0.03	1.89	0.07	0.04	0.00	0.18	0.01
Fe+++	-	0.45	0.02	0.41	0.02	0.36	0.02	0.36	0.02	-	-	-	-
HCO3-	-	903	14.80	995	16.30	970	15.90	897	14.70	95.80	1.57	53.70	0.88
SO4--	-	22.30	0.46	17.70	0.37	20.60	0.43	19.80	0.41	34.20	0.71	9.90	0.21
Cl-	-	18800	530.32	19300	544.43	13500	380.82	17300	488.01	11.40	0.32	6.30	0.18
I-	-	131	1.03	128	1.01	84	0.66	111	0.87	-	-	-	-
Br-	-	136	1.70	134	1.68	96	1.20	122	1.53	-	-	-	-
HBO3--	-	68.60	2.29	71.90	2.40	50.90	1.70	53.60	1.79	-	-	-	-
S--	-	<0.2	-	<0.2	-	<0.2	-	<0.2	-	-	-	-	-
Total Cation			580.05		566.98		402.16		517.57		2.59		1.28
Total Anion			550.60		566.19		400.71		507.31		2.60		1.27
Total Cation - Anion			29.45		0.79		1.45		10.26		-0.01		0.01
Ion balance equation*			2.60		0.07		0.18		1.00		-		-
SiO2	mg/l	70.0		73.0		64.0		61.0		32.3		32.5	
TOC	mg/l	82		67		100		69		-		-	
Humic acid	mg/l	104		123		74		47		-		-	
Fulvic acid	mg/l	75		74		178		66		-		-	
δ D	per mill	-0.4		1.9		-0.8		-3.2		-39.5		-40.0	
δ 18O	per mill	-1.93		-1.90		-2.61		-2.53		-6.80		-6.90	

** Note : Ion balance equation = (Total Cation - Total Anion) / (Total Cation + Total Anion) × 100*

Table 2 : Chemistry of groundwaters from the South Kanto gas field (data from Sugisaki et al., 1962)

Locality No.	Sampling Depth (m)	Atmospheric Temp (℃)	Groundwater Temp (℃)	pH	Na		K		Mg		Ca		NH4+		HCO3-		Cl-		Br-		I-	
					(meq/L)	(mg/L)	(meq/L)	(mg/L)	(meq/L)	(mg/L)	(meq/L)	(mg/L)	(meq/L)	(mg/L)	(meq/L)	(mg/L)	(meq/L)	(mg/L)	(meq/L)	(mg/L)	(meq/L)	(mg/L)
No.1	966	14.3	34.9	7.47	422	9706	5.8	226.78	12.9	156.86	8.46	169.54	6.90	124.20	10.38	633.28	458.7	16260.9	0.88	70.31	0.13	16.50
No.2	632	16.1	26.7	7.40	344	7912	6.4	250.24	23.7	288.19	10.09	202.20	10.00	180.00	7.53	459.41	386.2	13690.8	0.75	59.93	0.24	30.46
No.3	1150	11.1	30.8	7.38	381	8763	6.9	269.79	27.4	333.18	11.07	221.84	9.10	163.80	5.56	339.22	427.4	15151.3	0.81	64.72	0.28	35.53
No.4	2051	15.0	40.0	7.37	478	10994	7.4	289.34	25.5	310.08	17.07	342.08	11.60	208.80	4.64	283.09	538.8	19100.5	1.03	82.30	0.34	43.15
No.5	1305	16.6	34.6	7.47	468	10764	9.2	359.72	26.7	324.67	17.88	358.32	8.50	153.00	5.68	346.54	526.1	18650.2	1.24	99.08	0.36	45.68
No.6	970	17.5	28.9	7.38	422	9706	3.3	129.03	34.0	413.44	16.33	327.25	7.90	142.20	8.78	535.67	479.6	17001.8	1.01	80.70	0.28	35.53
No.7	1126	10.2	40.0	7.25	146	3358	2.3	89.93	12.4	150.78	16.80	336.67	2.50	45.00	5.33	325.18	218.5	7745.8	0.34	27.17	0.04	5.08
No.8	815	17.3	25.3	7.25	451	10373	9.6	375.36	45.1	548.42	16.50	330.66	12.30	221.40	7.48	456.35	532.6	18880.7	1.25	99.88	0.45	57.11
No.9	900	21.0	23.2	7.57	478	10994	9.6	375.36	50.4	612.86	11.10	222.44	11.00	198.00	11.96	729.68	548.4	19440.8	1.35	107.87	0.34	43.15
No.10	1711	19.6	32.9	7.50	576	13248	7.0	273.70	33.2	403.71	15.00	300.60	13.10	235.80	9.22	562.51	635.3	22521.4	1.21	96.68	0.54	68.53
No.11	1993	20.7	28.0	7.61	352	8096	5.6	218.96	30.2	367.23	9.35	187.37	4.90	88.20	12.54	765.07	412.7	14630.2	0.83	66.32	0.32	40.61
No.12	1224	11.5	28.5	7.32	484	11132	8.0	312.80	47.0	571.52	11.26	225.65	10.90	196.20	20.13	1228.13	551.5	19550.7	0.96	76.70	0.72	91.37
No.13	1050	14.1	26.4	7.35	468	10764	2.9	113.39	39.1	475.46	11.43	229.06	12.20	219.60	11.01	671.72	547.3	19401.8	1.29	103.07	0.79	100.25
No.14	1511	14.5	31.3	7.53	487	11201	3.5	136.85	33.8	411.01	13.36	267.73	10.10	181.80	15.53	947.49	548.4	19440.8	1.35	107.87	0.91	115.48
No.15	548	15.0	20.0	7.92	237	5451	4.4	172.04	20.7	251.71	3.68	73.75	5.20	93.60	18.84	1149.43	271.5	9624.7	0.71	56.73	0.44	55.84
No.16	437	12.8	15.8	7.66	457	10511	7.4	289.34	47.3	575.17	8.61	172.54	11.60	208.80	13.26	808.99	523.0	18540.4	1.20	95.88	0.78	98.98
No.17	1365	13.0	32.2	7.61	544	12512	6.4	250.24	25.7	312.51	12.98	260.12	12.40	223.20	18.93	1154.92	588.7	20869.4	1.18	94.28	0.94	119.29
No.18	1536	17.3	32.7	7.63	489	11247	6.3	246.33	26.1	317.38	14.55	291.58	9.70	174.60	14.58	889.53	548.4	19440.8	1.07	85.49	0.91	115.48
Average (all)		15.4	29.57	7.48	426.89	9818.44	6.22	243.29	31.18	379.12	12.53	251.08	9.44	169.90	11.19	682.57	485.7	17219.0	1.03	81.94	0.49	62.11

	Total Cation	Total Anion	Total Cation - Total Anion	Total Cation + Total Anion	Ion balance equation*	Predicted Groundwater Temp.
No.1	456.06	470.1	-14.03	926.15	-1.51	33.62
No.2	394.19	394.7	-0.53	788.91	-0.07	28.740
No.3	435.47	434.1	1.42	869.52	0.16	34.100
No.4	539.57	544.8	-5.24	1084.38	-0.48	56.020
No.5	530.28	533.4	-3.10	1063.66	-0.29	42.700
No.6	483.53	489.7	-6.14	973.20	-0.63	36.900
No.7	180.00	224.2	-44.21	404.21	-10.94	32.720
No.8	534.50	541.8	-7.28	1076.28	-0.68	33.600
No.9	560.10	562.1	-1.95	1122.15	-0.17	39.000
No.10	644.30	646.3	-1.97	1290.57	-0.15	53.820
No.11	402.05	426.4	-24.34	828.44	-2.94	60.560
No.12	561.16	573.3	-12.15	1134.47	-1.07	35.980
No.13	533.63	560.4	-26.76	1094.02	-2.45	35.100
No.14	547.76	566.2	-18.43	1113.95	-1.65	44.720
No.15	270.98	291.5	-20.51	562.47	-3.65	25.960
No.16	531.91	538.2	-6.33	1070.15	-0.59	21.540
No.17	601.48	609.8	-8.27	1211.23	-0.68	40.300
No.18	545.65	565.0	-19.31	1110.61	-1.74	48.020
Average	486.26	498.4	-	-	-	39.080

** Note : Ion balance equation = (Total Cation - Total Anion) / (Total Cation + Total Anion) ×100*

***Table 3** : Compositions of gases separated from groundwaters in the South Kanto gas field (data from Sugisaki et al., 1962)*

Locality No.	CH4(*g*)	CO2(*g*)	N2(*g*)	Ar(*g*)	C2H6(*g*)	H2(*g*)	He(*g*)
Unit	(%)						
No.1	96.70	1.560	1.750	0.0350	0.0210	0.00077	0.00009
No.2	95.40	1.730	2.860	0.0370	0.0130	0.00130	0.00086
No.3	97.30	2.360	0.290	0.0076	0.0067	0.00032	0.00057
No.4	97.80	1.830	0.384	0.0099	0.0060	-	-
No.5	96.60	0.855	2.290	0.0270	0.0800	0.00084	0.00043
No.6	98.90	0.842	0.292	0.0062	0.0120	0.00130	0.00078
No.7	97.40	1.890	0.650	0.0730	0.0090	0.00540	0.00650
No.8	98.50	0.904	0.557	0.0120	0.0030	0.02400	0.00074
No.9	98.70	1.110	0.167	0.0028	0.0030	0.00090	0.00002
No.10	98.40	1.310	0.296	0.0060	0.0070	0.00090	0.00025
No.11	97.80	1.360	0.870	0.0160	0.0060	0.00200	0.00055
No.12	97.10	2.700	0.170	0.0033	0.0070	0.00033	0.00051
No.13	98.40	1.410	0.231	0.0046	0.0250	0.00083	0.00001
No.14	97.60	2.050	0.370	0.0081	0.0010	0.00049	0.00016
No.15	98.60	0.364	0.986	0.0160	0.0080	0.00340	0.00001
No.16	99.00	0.393	0.561	0.0140	0.0180	0.00220	0.00001
No.17	94.00	-	4.960	0.0500	-	-	-
No.18	89.50	1.240	9.300	0.0960	0.0062	-	-

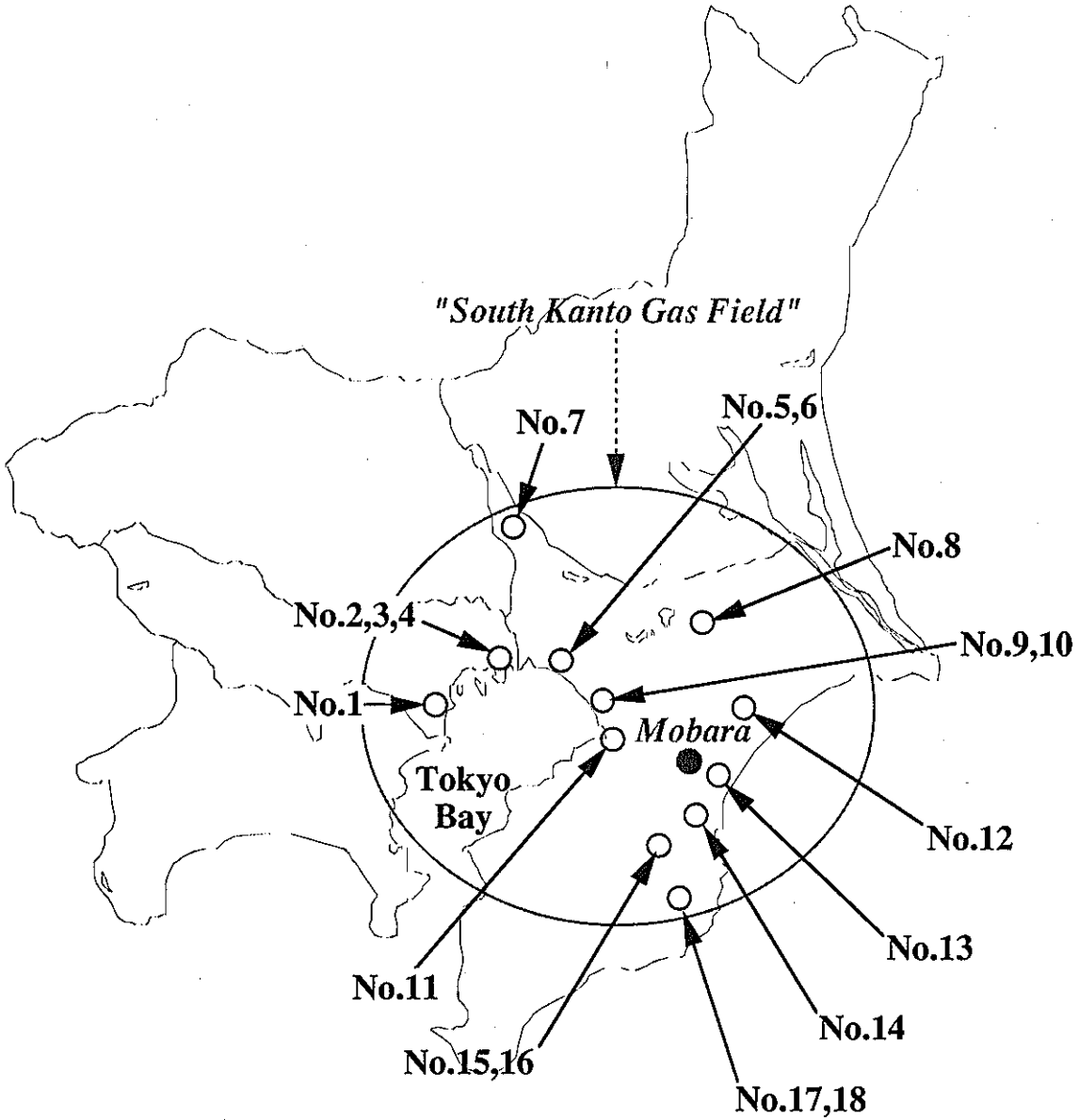

Borehole Name:

No.1 : Omori-Heiwajima
No.2 : Koto ER10-A
No.3 : Koto ER10-B
No.4 : Koto ER10-C
No.5 : Funabashi FR-10
No.6 : Funabashi FR-11
No.7 : Otone Spring
No.8 : Narita No.2
No.9 : Chiba
No.10 : Fuji boring FR-2
No.11 : Yahata K-6
No.12 : Yokoshiba Y-13
No.13 : Togane R-2
No.14 : Nichiten NR-1
No.15 : Tosho T-12
No.16 : Kanhatsu SRT-13
No.17 : Aio 615
No.18 : Aio 617

***Figure 4**: Location of gas wells in the South Kanto gas field (from Sugisaki et al., 1962)*

suggesting that the effect of drilling fluids on groundwater compositions should be minimal. The groundwaters were sampled at the wellhead, where physico-chemical parameters (*e.g.*, temperature, pH, Eh *etc.*) were immediately determined (Kamei *et al.*, 2000). The chemistry of the groundwaters was determined by ion chromatography (Cl^-, SO_4^{2-}), atomic absorption spectrometry (Ca, Mg, Fe), flame spectrometry (Na, K), iodometric titration (Br^-, I^-), absorption spectrophotometry (S^{2-}, SiO_2, humic acid, fulvic acid) and volumetry (B). Isotopic ratios (δ D, $\delta\ ^{18}O$) were determined by mass spectrometry.

Charge-balance errors for the four groundwater samples (sampling points; No.78, No.98, SK-2 and M-10) and 2 surface water samples (sampling points; SW-1 and SW-2) in Table 1 were calculated using the following equation (Friedman and Erdmann, 1982):

$$Charge\ balance = \frac{[\sum Cation(meq/L) - \sum Anion(meq/L)]}{[\sum Cation(meq/L) + \sum Anion(meq/L)]} \times 100$$

This equation is appropriate for total anion concentrations between 10 and 800 meq/l. If the calculated charge balance lies within $\pm$ 2 to 5%, the quality of the analysis is considered acceptable. The calculated charge balances for all the samples noted above are between 0.07% and 2.60%, and the quality of the analyses for these samples are therefore acceptable. Similar calculations for the South Kanto gas field samples (Table 2), range from -10.94% to 0.16%. The worst charge-balance error occurs for sample No.7, and this analysis was therefore rejected. Charge balances for the remaining samples are acceptable because they lie between $\pm$ 2 to 5%. A deficiency of positive charge is calculated for most samples.

The deuterium and ^{18}O ratios of rainwater and snowmelt in Japan generally lie in a range bounded by two straight lines (δ D = 8 $\delta\ ^{18}O$ +10 and δ D = 8 $\delta\ ^{18}O$ +26), with δ D = -40 to -100‰ (Matsubaya, 1985). Deuterium and ^{18}O ratios of surface-water samples from the Mobara area plot in this range (Figure 5). Deuterium and ^{18}O ratios of groundwaters from the Mobara area are, however, similar to those of sea water (δ D = 0, $\delta\ ^{18}O$ = 0). The Kazusa group is primarily marine in origin, and it is therefore possible that connate seawater, possibly modified by water-rock interactions, exists in the pore spaces of these sedimentary rocks. If so, these groundwaters may be as old as the Neogene. Isotopic data (*e.g.*, tritium or ^{14}C concentrations) that could be used to test this possibility are unavailable.

Although the δ D values of groundwaters from the Mobara area are similar to those of seawater, $\delta\ ^{18}O$ values are slightly depleted in comparison with seawater. The depth of the

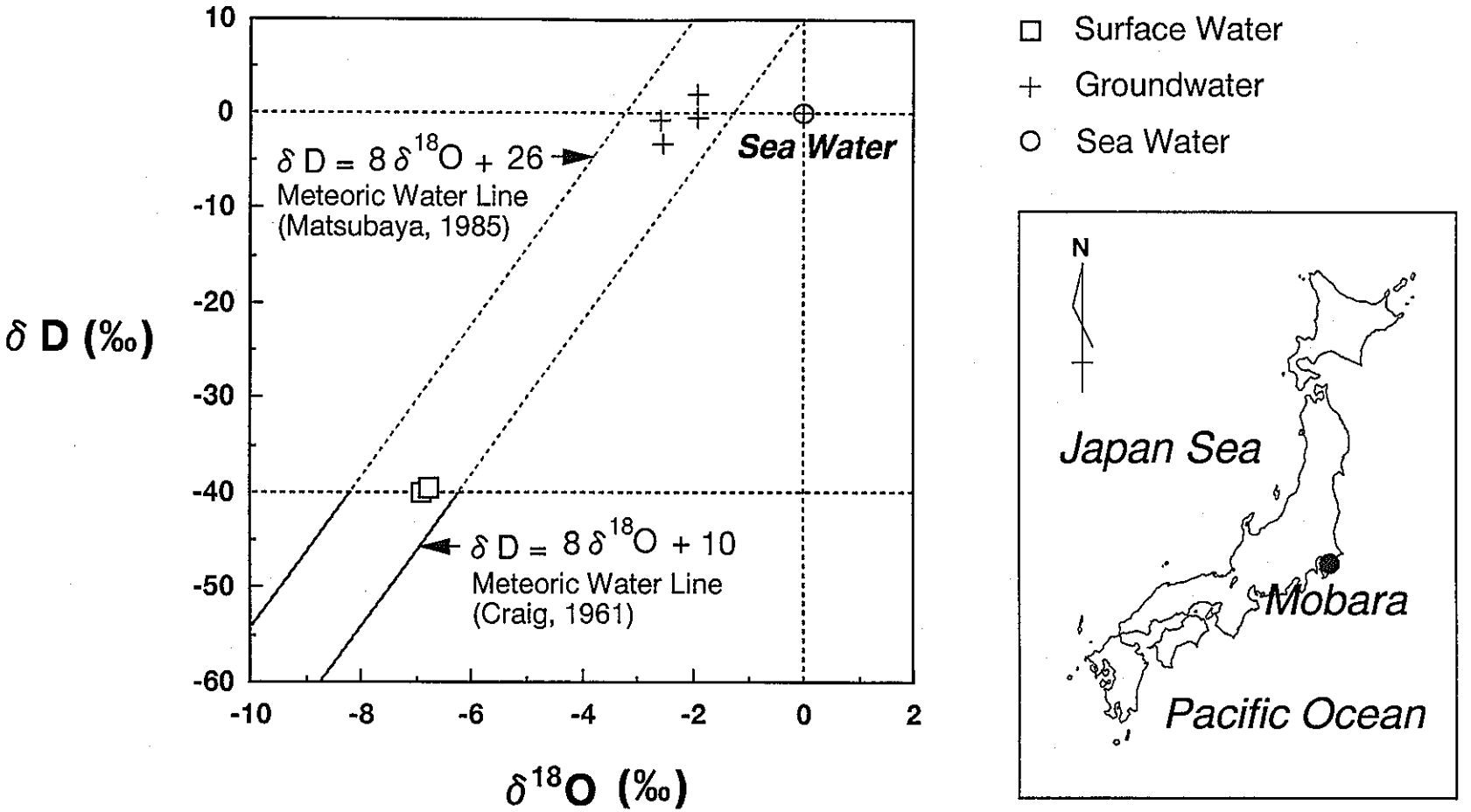

***Figure 5**: Deutrium and 18-oxygen data for surface waters and groundwaters at Mobara area*

water table in this area is about 150 m below the surface (Nirei, 1993). Strainers, about 500 m length (see Table 1), are emplaced in each well below the water table. Because the strainers are installed over a significant length of the well bore, it is possible that dilute surface waters may have mixed with deeper groundwaters.

This possibility is consistent with $\delta^{18}O$ values measured in Mobara groundwaters. In general, if the groundwater is strongly affected by rock-water interaction, the $\delta^{18}O$ of the groundwater is enriched. In samples of Mobara groundwater, however, the $\delta^{18}O$ of the groundwater is slightly depleted relative to sea water. This may indicate that the groundwater is affected by mixing with surface water. Such mixing is also indicated by Cl^- concentrations in Mobara groundwaters (13,500 to 19,300 mg/L), which are slightly less than Cl^- concentrations in seawater (about 19,892 mg/L; Drever, 1988).

The pH of groundwaters sampled from the Mobara area is about 8 (7.74 to 7.94). Measured Eh values (*vs.*SHE) in groundwaters sampled at the wellhead are about -50 mV (-73 to -34 mV). Motojima and Hirukawa (1979) report a similar range of Eh values (-50 to -100 mV) for Mobara groundwaters.

Figure 6 shows the range of ionic concentrations measured in Mobara groundwaters. The groundwater is a Na-Cl type solution. Normalization of the compositions of these groundwaters to that of seawater (Figure 7) suggests that they are similar to seawater, but the concentrations of several solutes differ significantly. These differences include:

- Na^+ and Cl^- concentrations in Mobara groundwaters are of the same order, or slightly depleted, compared to seawater.
- Ca^{2+}, Mg^{2+}, SO_4^{2-} concentrations are less than those of seawater.
- K^+, HCO_3^-, I^-, Br^-, HBO_3^{2-}, $SiO_2(aq)$ concentrations are greater than those of seawater.

The high concentrations of K^+ and I^- in Mobara groundwaters are noteworthy. These concentrations are greater than those of groundwater samples from the South Kanto gas field (Table 2). High concentrations of iodine have been measured in both the rocks and groundwaters of the Mobara area (Motojima and Hirukawa, 1979). Motojima and Hirukawa (1979) suggest that the high I^- concentrations originate from seaweed and diatoms. These biological materials also contain high concentrations of K^+, suggesting that they are the source of elevated K^+ concentrations Mobara groundwaters.

The slightly elevated concentrations of HCO_3^- (897 to 995 mg/L) relative to seawater in

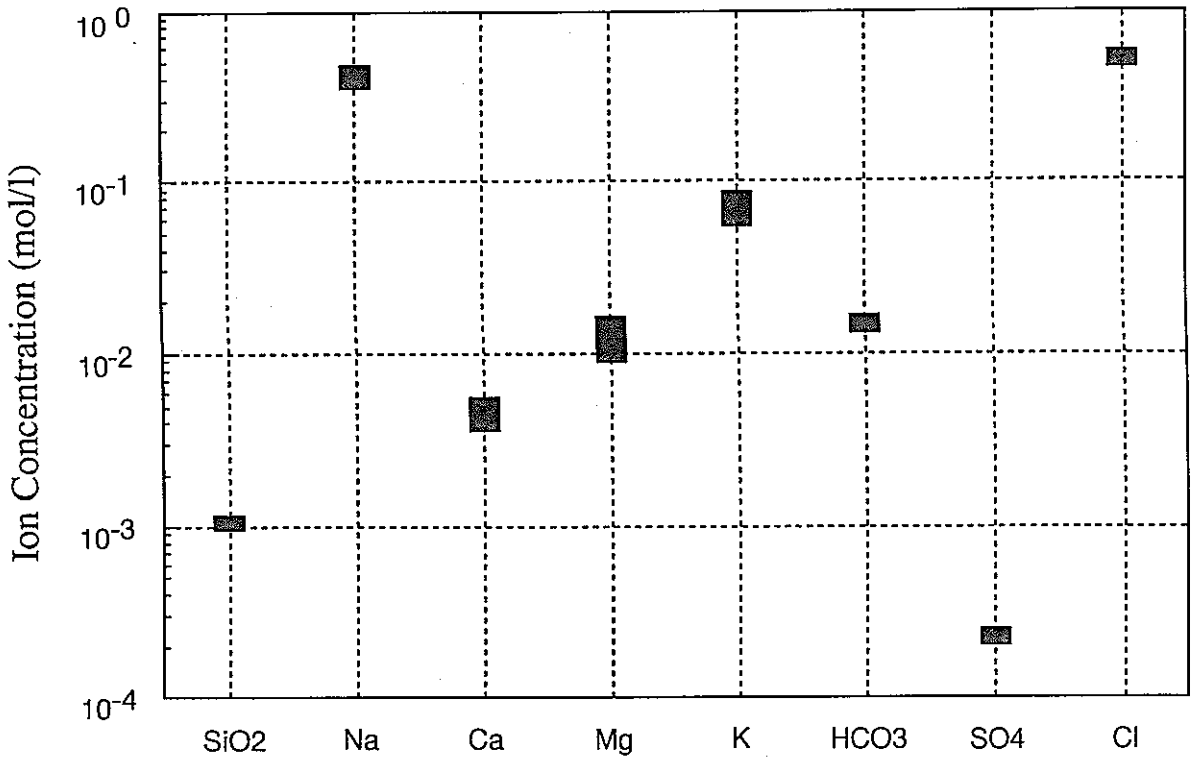

***Figure 6**: Chemistry of groundwaters from the Mobara area*

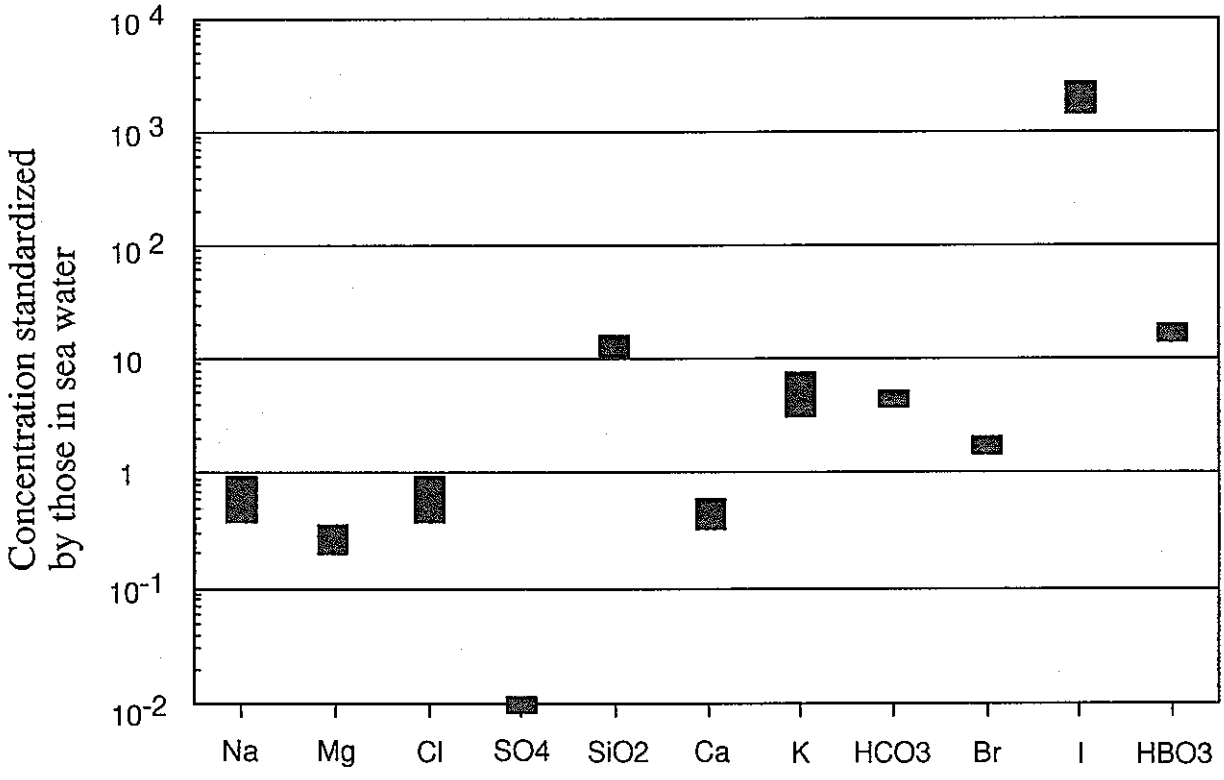

***Figure 7**: Mobara groundwater compositions standardized to that of sea water*

Mobara groundwaters are typical of groundwaters from natural gas regions (Motojima and Hirukawa, 1979). The low concentrations of SO_4^{2-} (17.7 to 22.3 mg/L) relative to seawater are slightly higher than corresponding values reported by Motojima and Hirukawa (1979) [0.7 to 1.1 mg/l]. Concentrations of SO_4^{2-} in connate groundwaters are generally low because SO_4^{2-} is reduced via bacterially mediated reactions to H_2S, S and FeS (*e.g.*, Ii *et al.*, 1997). As noted above, however, the Eh of Mobara groundwaters is only slightly reducing, which may indicate that the Eh measurements are affected by contact with air during sampling and/or prior to measurement.

The concentrations of humic substances in the Mobara groundwater are very high. The concentration of dissolved organic carbon (DOC) in groundwaters is typically about 0.5 mg/l, and most of the DOC is in the form of humic and fulvic acids (Drever, 1988). The concentrations of humic acid in Mobara groundwaters range from 47 to 123 mg/L, and concentrations of fulvic acid range from 66 to 178 mg/L (Kamei *et al.*, 2000). Sugisaki *et al.* (1963) suggest that $CH_4(g)$, the predominant gas produced from wells in the Mobara area, may be generated by bacterial fermentation reactions. The high concentrations of humic and fulvic acids in Mobara groundwaters are consistent with this suggestion, but measured Eh values, as noted above, appear to be too oxidizing. The simplest, and one of the most important, bacterial fermentation reaction generating methane [*e.g.*, $2C_{organic} + 2H_2O = CO_2(g) + CH_4(g)$] requires a lower redox potential (*e.g.*, pe equals about -4, at pH equals around 7 and 25℃; Drever 1988) than measured. As noted above, groundwater samples collected at the wellhead may have been oxidized by contact with air, in which case the measured Eh values would not be a reliable indicator of redox conditions in the subsurface environment.

2.2.3 Mineralogy of Otadai Formation

Kamei *et al.* (2000) characterized the mineralogy of the argillaceous Otadai formation using XRD techniques. The mineralogy includes:

quartz > plagioclase > montmorillonite, chlorite, calcite > illite, α-tridymite, K-feldspar, clinoptilolite, pyrite, siderite, hornblende

Non-clay minerals, particularly quartz and plagioclase, are thus important components of the Otadai formation.

2.3 Thermodynamic Interpretation of Groundwater Chemistry

The REACT module of the Geochemist's Workbench geochemical modeling software package (Bethke, 1996) was used to calculate the concentration distribution of aqueous species in groundwaters and surface waters of the Mobara area and South Kanto gas field. Mineral saturation states were calculated based on the results of the aqueous-speciation calculations. Mineral saturation states indicate whether the respective minerals are equilibrated with the groundwaters, or whether the minerals should dissolve or precipitate. The so-called B-dot model was used to calculate ionic activity coefficients. This model, which is based on the extended Debye-Huckel equation, is appropriate for solutions with ionic strengths less than about 1 molal. The model is appropriate for Mobara groundwaters because the ionic strength of these solutions is less than that of seawater (approximately 0.65 molal).

The chemical analyses in Tables 1 and 2 are reported in units of mg/L. REACT requires values for the solution's density and Total Dissolved Solids (TDS) content if analyzed concentrations are in these units. An iterative calculation procedure described by Bethke (1996) was used to estimate the density and TDS content of the samples noted in Tables 1 and 2. This procedure is described in Appendix A.

Calculated saturation indices for calcite and dolomite in Mobara groundwaters and surface waters, and South Kanto gas field groundwaters are summarized in Figure 8 (sample No.7 from the South Kanto gas field is excluded from the calculations because the charge balance error for this sample is unacceptable, see Section 2.2). The saturation index (SI) is given by:

$SI = \log (IAP/K)$,

where IAP denotes the Ion Activity Product and K refers to the equilibrium constant. Equilibrium is indicated when $SI = 0$. If $SI > 0$, then the groundwater is supersaturated (*i.e.*, precipitation is required to achieve equilibrium), and if $SI < 0$, then the groundwater is undersaturated (dissolution is required to achieve equilibrium).

There are several sources of uncertainty in calculations of the saturation index, including errors in chemical analyses, uncertainties in the equilibrium constant and uncertainties in methods used to calculate ionic activities. To deal with these uncertainties, a range of saturation index values, centered on a value of zero, is generally taken to indicate equilibrium.

Langmuir (1997) adopted a range of SI values for calcite equal to 0 ± 0.1 (at best). This range is also adopted in the present study.

As can be seen in Figure 8, groundwaters in the Mobara area and the South Kanto gas field are supersaturated with respect to calcite. The SI values for calcite range from 0.204 (sample No.8) to 1.00 (sample No.78). An SI value greater than zero may indicate that the mineral is kinetically inhibited from precipitating. Calcite is known to equilibrate relatively quickly with aqueous solutions at low temperatures and this mineral is present in the Otadai formation (see Section 2.2.3), however. Values greater than 0 for the saturation index of calcite may therefore be due to errors in the chemical analyses of the Mobara groundwaters. This possibility is evaluated in Section 2.4.2.3.

Groundwaters from the Mobara area are also supersaturated with respect to siderite (SI = 0.49 to 0.84) and dolomite [S.I. = 1.95 (sample No. 3) to 3.51 (sample No. 98)]. Like calcite, siderite is present in the Otadai formation and may precipitate relatively quickly as a pure phase or in a carbonate solid solution. Dolomite precipitation is not observed over laboratory time scales (e.g., Drever, 1988), and this mineral is not present in the Otadai formation. The absence of dolomite would suggest that calculated S.I. values for this mineral should be less than zero, in conflict with the results noted above. This observation may suggest that the groundwater analyses are in error, or that dolomite fails to precipitate for kinetic reasons over time scales that are at least as long as the residence time of Mobara groundwaters in the Otadai formation.

It is extremely difficult to obtain stable and reproducible Eh measurements in the field. As noted in Section 2.2.2, we suspect that the Eh measurements for the Mobara-area groundwaters may have been disturbed by contact of the samples with atmospheric oxygen. To evaluate this possibility, Eh values were calculated using the "decouple" command in REACT and measurements of total Fe(II) and Fe(III) concentrations in the groundwaters (Table 1). Results thus represent the Eh corresponding to the iron oxidation reaction ($Fe^{3+} + e^- = Fe^{2+}$), and are summarized in Table 4.

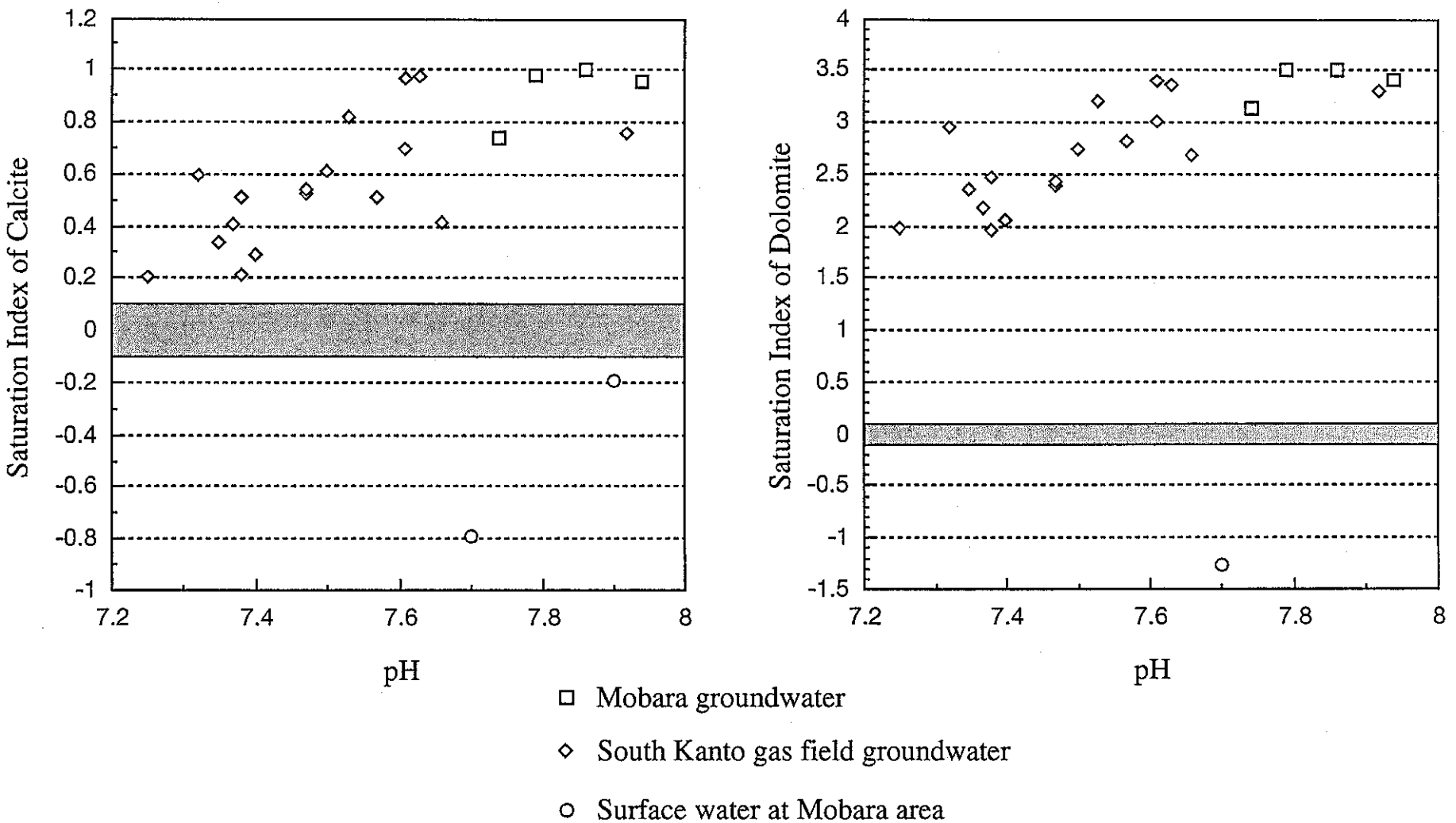

***Figure 8**: Saturation indices for calcite and dolomite in Mobara groundwaters, Mobara surface waters and South Kanto gas-field groundwaters*

Table 4: Comparison of measured Eh measured values with Eh values calculated assuming equilibrium for the iron-oxidation reaction.

	Measured Values	Calculated Values
No.78	-50 mV	98 mV
No.98	-34 mV	82 mV
SK-2	-73 mV	94 mV
M-10	-52 mV	107 mV

As can be seen, the calculated values are consistently more oxidizing than the measured values. This suggests that these groundwaters are not in redox equilibrium with respect to the iron oxidation reaction, assuming that the measured values are correct.

2.4 Corrections to Chemical Analyses of Mobara Groundwaters

As noted in Section 2.2.2, samples of the Mobara-area groundwaters may have been contaminated, or altered, during sampling. Degassing could have altered the compositions of samples collected at the surface relative to their *in-situ* compositions. We suspect that such degassing may be important because samples of the Mobara-area groundwaters were extracted from deep gas wells, and because large amounts (several hundred m^3 per day) of various gases were separated at the surface. As noted in similar studies of deep groundwaters in Switzerland (Nagra, 1989): "*Temperature and pressure changes during sampling can affect chemical equilibria in the groundwater. In general, dissolution or precipitation processes do not occur so quickly that the groundwater chemistry is altered significantly unless sampling occurs very slowly or at very high formation temperatures. However, the situation is different from potential degassing of the water resulting from a drop in pressure as the sample is extracted from the borehole. This can occur very rapidly and affects mainly the carbonate system in the groundwater*".

Considerable effort in the present study has therefore been devoted to assessing whether the effects of degassing could have altered the chemistry of the Mobara groundwater samples, and, if so, to develop and apply geochemical modeling techniques to correct the samples for the effects of degassing. The results of this effort are described in the following sections.

2.4.1 Sampling Conditions

Gas wells in the Mobara area are referred to as the "*Mobara type*" (Natori, 1997), which indicates a type of well from which a particularly high ratio of gas-to-water is produced. The range of the gas-to-water ratio produced from this type of well is fairly wide. For example, the ratio varies from 0.45 to 59.7 in the South Kanto gas field (Sugisaki *et al.*, 1963). The production depth in this field ranges from 500 to 2000 m. The pressure at these depths is hydrostatic, at least during early stages of gas production (Natori, 1997). The hydrostatic pressure ranges from 50 kgf/cm^2 to 200 kgf/cm^2. If such highly pressurized groundwaters are sampled at the wellhead, the effects of degassing on physico-chemical parameters (pH, Eh) may be significant (Arthur and Murphy, 1989).

Kamei *et al.* (2000) do not report gas compositions and gas-to-water ratios measured at the wellhead for the groundwater samples considered in their study. The gas-to-water ratio was therefore estimated using the following equation:

$$Gas/Water\ ratio = \frac{amount\ of\ generated\ gases\ (m^3/day)}{amount\ of\ water\ out\ flow\ (m^3/day)},$$

and data characterizing the water outflow rate (m^3/day), amount of generated gases (m^3/day), and gas compositions for the South Kanto gas field from Sugisaki *et al.* (1963).

2.4.2 Correction Method to Estimate In-situ Groundwater Chemistry

The conceptual model used to correct analyses of the Mobara-area groundwaters for the effects of degassing is illustrated schematically in Figure 9. Gases separated at the wellhead that may affect physico-chemical parameters, such as the pH and Eh, are $CH_4(g)$ and $CO_2(g)$. Degassing of $CO_2(g)$ will cause the pH to increase in accordance with the following reactions:

$$CO_2(g) + H_2O \Leftrightarrow H_2CO_3 \Leftrightarrow H^+ + HCO_3^-$$

The rate of the hydration/dehydration reaction is sufficiently fast at 25℃ that only a few minutes are necessary to establish equilibrium (Stumm and Morgan, 1981).

Degassing of $CH_4(g)$ may affect the redox potential of a groundwater sample according to the

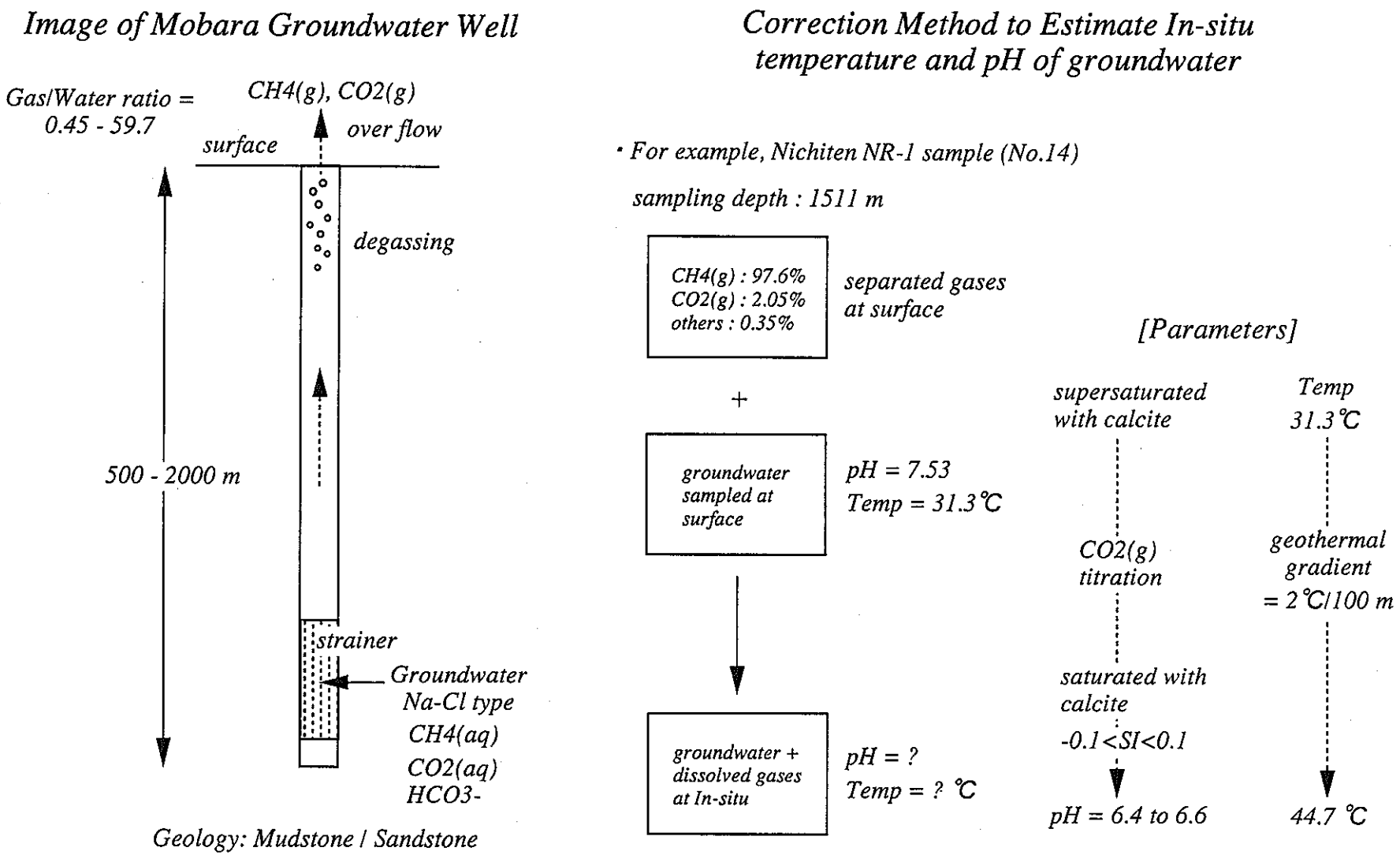

***Figure 9**: Schmatic diagram of a groundwater well in the Mobara area, and illustration of the correction method to estimate in-situ groundwater chemistry*

following reaction:

$$CH_4(g) + 2H_2O \rightarrow 8H^+ + CO_2(g) + 8e^-.$$

This half-cell reaction is included in the following overall reaction (Stumm and Morgan, 1981):

$$CH_3COOH \rightarrow CH_4(g) + CO_2(g),$$

which indicates that methane may be formed directly from acetic acid. The rate of this reaction is extremely slow (Stumm and Morgan, 1981), however, which suggests that degassing of $CH_4(aq)$ should not affect the Eh of groundwater samples. Other gases, including N_2, Ar, and H_2, are also not expected to affect the Eh or pH of Mobara groundwaters because they occur in trace amounts, or are inert.

Based on the above considerations, the *in-situ* chemistry of a groundwater sample from the Nichiten NR-1 gas well in the South Kanto gas field (data from Sugisaki *et al.*, 1963) was estimated by simulating the effects on groundwater chemistry of $CO_2(g)$ and $CH_4(g)$ degassing at the wellhead. The location of this well (corresponding to sample No.14, Figure 4) is close to the Mobara area. It may therefore produce gases that are similar in composition to gasses produced from Mobara gas wells. The relevant data from sample No. 14 are as follows:

- Gas composition (separated at the surface); CH_4 = 97.6 %, CO_2 = 2.05%, others = 0.35%, and
- Gas/water ratio; 2500 (m^3/day)/1300 (m^3/day) = 1.93

Other data and techniques used in the simulation procedure to estimate the *in-situ* composition of this sample are described in the following sections.

2.4.2.1 In-situ Temperature

Groundwater temperature increases with depth due to the geothermal gradient. Although the rate of groundwater flow from producing horizons to the wellhead is fast in Mobara wells, the temperature of samples at the surface may nevertheless be less than the *in-situ* temperature. Constraints described in the following paragraphs were used to estimate the *in-*

situ temperature, assuming static groundwater flow conditions.

The temperature of surface waters from the Mobara area is about 14.7℃. The temperature of groundwaters sampled at the surface varies from 24 to 28.6℃ (average = 26.3℃; Kamei *et al.*, 2000). The average geothermal gradient in the area is about 2℃/100m (Chiba Prefecture Research Institute for Environmental Pollution, 1982).

Packers are not installed in the wells, so exact locations where the groundwater flows into the borehole from the surrounding rock mass is unknown. We assume that the sampling depth is the median depth between the upper and lower strainer depths. Median depths for the Mobara-area wells (Table 1) are as follows:

No.78 = Median depth: G.L. -1081m (Strainer depth: G.L. -960 to -1202m)
No.98 = Median depth: G.L. -1098m (Strainer depth: G.L. -895 to -1301m)
SK-2 = Median depth: G.L. -929m (Strainer depth: G.L. -717 to -1140m)
M-10 = Median depth: G.L. -733m (Strainer depth: G.L. -517 to -949m)
where, G.L. is the abbreviation of *"Ground Level"*.

Based on the surface temperature, geothermal gradient, and median depths to sampling horizons, we estimated the *in-situ* groundwater temperature as follows:

No.78: 14.7℃ + 2℃/100m×1081m = 36.3℃ (33.9 to 38.74℃ for the upper and lower strainer depths, respectively)
No.98: 14.7℃ + 2℃/100m×1098m = 36.7℃ (32.6 to 40.7℃ for the upper and lower strainer depths, respectively)
SK-2: 14.7℃ + 2℃/100m×929m = 33.3℃ (*i.e.*, 29.0 to 37.5℃ for strainer depth, respectively)
M-10: 14.7℃ + 2℃/100m×733m = 29.4℃ (*i.e.*, 25.0 to 33.7℃ for strainer depth, respectively)

The average *in-situ* temperature is 33.9℃, which is about 7℃ higher than the average sampling temperature measured at the surface.

In-situ temperatures for groundwaters from the South Kanto gas field were also estimated using the above procedure (Table 2). Results range from 21.5℃ to 60.6℃. The average *in-situ* temperature is 39.1℃, which is about 10℃ higher than the average temperature

measured at the surface. The estimated *in-situ* temperatures for the Omori-Heiwajima sample (No.1) and Otone-Spring sample (No.7) are 33.6℃ and 32.7℃, respectively, which are lower than values measured at the surface (34.9℃ and 40.0℃, respectively), This suggests that the geothermal gradient in the vicinity of these two wells may be greater than 2℃/100m [the average geothermal gradient in Japan is 3℃/100m (Rikitake, 1992)].

2.4.2.2 Partial Pressure of Gas in Groundwater

The solubility of a gas in aqueous solution is proportional to the partial pressure of the gas, in accordance with Henry's law. It is therefore possible to calculate the partial pressure of a gas based on its concentration in the aqueous phase. To estimate the *in situ* partial pressures of gases in a groundwater sample, we assume that gases separated at surface dissolve completely back into the sample. The amount of the separated gases is calculated from the gas/water ratio using the perfect gas law. The calculation procedure is described in the following paragraphs, using data for sample No.14 of the South Kanto gas field as an example. Results using this procedure for groundwaters from the South Kanto gas field are summarized Table 5.

According to the perfect gas law (*i.e.*, $PV = nRT$; where P stands for pressure, V denotes volume, n refers to the number of moles of gas, R stands for the gas constant and T represents absolute temperature), a change in V can be calculated for a given change in pressure or the absolute temperature. For one mole of a perfect gas, the corresponding volume is 22.41 L at 0℃. The volume at 44.7℃ (*i.e.*, the estimated *in-situ* temperature for sample No. 14) is 26.07 L. The gas-to-water ratio for sample No. 14 is 1.93, which means that 1.93 m^3 gases is dissolved in 1.0 m^3 water under *in-situ* conditions. The separated $CH_4(g)$ concentration is then estimated as follows:

$1.93\ m^3 \times 0.976 = 1.88368\ m^3 = 1883.68\ L,$
$1\ mol : 26.07\ L = x : 1883.68\ L,$
$x = 72.255\ mol,$

and 72.255 mol of $CH_4(g)$ is therefore dissolved in 1 m^3 H_2O under *in-situ* conditions.

We assume that $CH_4(g)$ dissolves completely back into the groundwater, and that the dissolved species exists only as $CH_4(aq)$. The Henry's law constant for $CH_4(g)$ is 1.30×10^{-3} mol/L bar at 44.7℃, so the partial pressure of $CH_4(g)$ is given by;

***Table 5** : Calculated amounts of gaseous CH4 and CO2 separated from groundwater samples from the South Kanto gas field*

Locality No.	Gas/Water[1)]	CO_2 (g)[1)]	CH_4 (g)[1)]	CH_4 (molal)[2)]	CO_2 (molal)[2)]
No.1	1.68	1.560	96.7	6.431E-02	1.037E-03
No.2	2.69	1.730	95.4	1.037E-01	1.880E-03
No.3	2.01	2.360	97.3	7.762E-02	1.883E-03
No.4	2.20	1.830	97.8	7.971E-02	1.491E-03
No.5	2.00	0.855	96.6	7.459E-02	6.602E-04
No.6	1.90	0.842	98.9	7.390E-02	6.292E-04
No.7	0.45	1.890	97.4	1.707E-02	3.312E-04
No.8	2.80	0.904	98.5	1.096E-01	1.006E-03
No.9	1.00	1.110	98.7	3.856E-02	4.336E-04
No.10	2.20	1.310	98.4	8.074E-02	1.075E-03
No.11	1.80	1.360	97.8	6.433E-02	8.945E-04
No.12	1.52	2.700	97.1	5.822E-02	1.619E-03
No.13	1.83	1.410	98.4	7.124E-02	1.021E-03
No.14	1.93	2.050	97.6	7.226E-02	1.518E-03
No.15	39.50	0.364	98.6	1.588E+00	5.862E-03
No.16	59.70	0.393	99.0	2.446E+00	9.079E-03
No.17	2.00	-	94.0	7.314E-02	-
No.18	3.80	1.240	89.5	1.291E-01	1.789E-03
Average(All)	7.28	1.410	97.1	2.901E-01	1.895E-03
Average (Except for No.15 and 16)	2.38	1.400	94.7	8.577E-02	1.447E-03

Note

1) Gas/water ratio and gases data are derived from Sugisaki et al. (1963)

2) The gases dissolve in 1 liter of H_2O.

$(72.255 \times 10^{-3}$ mol/L) ÷ $(1.30 \times 10^{-3}$ mol/L bar) = 55.58 bar, *i.e.*, log $P_{CH4} = 1.74$

A similar procedure is used to estimate the amount of separated $CO_2(g)$ that dissolves back into the groundwater under *in-situ* conditions, *i.e.*:

$1.93\ m^3 \times 0.0205 = 0.039565\ m^3 = 39.565$ L,
1 mol : 26.07 L = x : 39.565 L,
$x = 1.518$ mol,

and 1.518 mol of CO_2 dissolves in 1 m^3 H_2O.

As $CO_2(g)$ dissolves in water, however, it produces dissolved $CO_2(aq)$ and other inorganic carbon species, including H_2CO_3, HCO_3^- and CO_3^{2-}. Henry's law constant cannot be applied directly to calculate the partial pressure of $CO_2(g)$ because other carbonate species are formed, and their concentration distribution depends on pH. A procedure to calculate the *in-situ* partial pressure of $CO_2(g)$, taking into account the aqueous speciation of dissolved carbonate species, is described in the following section.

2.4.2.3 Modeling the Carbonate System in Mobara Groundwaters

The total carbonate concentration is an important determinant of the hydrochemical properties of groundwater. As noted in the previous section, when $CO_2(g)$ is dissolved in water, carbonic acid (H_2CO_3), bicarbonate (HCO_3^-), carbonate (CO_3^{2-}) are formed. The concentrations of these aqueous species depend primarily on the total dissolved carbonate concentration, temperature and pH. Calculation of the concentrations of these species from chemical analyses of groundwaters sampled from deep boreholes is difficult because their concentrations are very sensitive to pressure and temperature variations, which are practically inevitable during sampling (*e.g.*, Nagra, 1989). Although special sampling devices may be employed to minimize the effects of such variations, a certain amount of CO_2 degassing may nevertheless occur. Degassing of $CO_2(g)$ may cause the pH to increase, resulting in a reduction of the CO_2/HCO_3^- concentration ratio.

The saturation index for calcite calculated from a chemical analysis of a groundwater from which some $CO_2(g)$ has degassed may be greater than zero due to the shift in pH to higher

values than exist under *in-situ*, or undisturbed conditions. Such calculations would incorrectly indicate that the *in-situ* groundwaters are supersaturated with respect to calcite. Other potential sources of error in calcite SI calculations include differences in temperature between the point of sampling and the *in-situ* temperature, and mixing of waters within the borehole or in the formation (Langmuir, 1997).

Nordstrom and Ball (1989) carried out a detailed examination of potential reasons leading to the apparent supersaturation of calcite (and other minerals) in deep groundwaters near the Stripa mine, Sweden. The sensitivity of the calculated SI values for calcite was evaluated in relation to errors in the chemical analyses and uncertainties in the thermodynamic data for calcite and dissolved carbonate species. Nordstrom and Ball (1989) concluded that the calculated supersaturation of the groundwaters with respect to calcite by nearly one-half an order of magnitude is a real effect that cannot be accounted for by errors in the analytical and thermodynamic data. These authors attributed the observed supersaturation to the relatively slow rate of calcite precipitation, or to solid-solution effects. The compositions of calcites from the Stripa area were found to be rather pure, however, suggesting that kinetic effects are the most likely explanation.

A kinetic contribution to the apparent supersaturation of many deep groundwaters with respect to calcite may not generally important, however, because the rate of calcite precipitation may be sufficiently rapid to achieve equilibrium if the residence time of the groundwater in contact with its host rocks is long. We believe this may be the case for Mobara-area groundwaters because calcite is present in the Otadai formation (Section 2.2.3) and because groundwaters in this formation appear to be connate solutions that have been slightly modified by water-rock interactions and/or mixing with more dilute surface waters (Section 2.2.2). As noted in Section 2.3, Mobara groundwaters are supersaturated with respect to calcite (saturation indices: 0.204 to 1.00, Figure 8), and the chemistry of these solutions may have been altered due to a pressure drop between the production horizon and the wellhead.

To correct the chemistry of groundwater samples from the Mobara area for the possible effects of degassing, we first assume that the *in-situ* groundwaters are saturated with respect to calcite (see Figure 9). A *back-titration* geochemical model is then used to simulate the addition of $CO_2(g)$ back into the sample, leading to an increase in the total carbonate concentration, and a decrease in pH. The end-point of the titration is taken to coincide with a calculated SI value for calcite = 0 ± 0.1. The uncertainty is assumed to represent the

cumulative uncertainty due standard errors in the chemical analyses, and to uncertainties in the thermodynamic data for calcite and dissolved carbonate species. It should be emphasized that a rigorous evaluation of the cumulative uncertainty has not been carried out in the present study, however. It is also assumed that mineral precipitation does not occur during the back-titration process. The effects of pressure variations are not considered because such effects are insignificant at pressures less than a few hundred atmospheres (*e.g.*, Ellis and McFadden, 1972).

2.4.3 Results of the Back-Titration Simulations

2.4.3.1 Test Case

The back-titration technique was tested based on the chemical analysis for sample No.14 from the South Kanto gas field (Table 2). The technique simulates the titration of an excess of $CO_2(g)$ (0.01 mol) into this sample, and corresponding variations in the SI value for calcite and pH are calculated. The *in-situ* pH corresponds to the titration end point, given by SI (calcite) = 0 ± 0.1. The REACT input script for the $CO_2(g)$ back titration simulation is provided in Appendix B.

Results of the simulation for sample No. 14 at 44.7℃ (*i.e.*, the *in-situ* temperature for this sample, see Section 2.4.2.1) are shown in Figure 10. As can be seen, calculated SI values for calcite decrease from an initial value of 1.0 to 0 at equilibrium. The amount of reacted $CO_2(g)$ is about 0.0055 mole/kg H_2O at the end point of the titration (the amount is about 0.0043 mol/kg for SI = 0.1, and about 0.007 mole/kg 0.0043 mole/kg for SI = -0.1). Corresponding changes in pH are shown in Figure 11. The pH decreases from an initial value of 7.53 to about 6.5 at SI (calcite) = 0. The pH at SI = -0.1 is 6.4 and at SI = 0.1 it is about 6.6. Resultant log P_{CO2} values change gradually (Figure 12), increasing from -1.79 (initial value) to -0.62 (calcite equilibrium). The log P_{CO2} at SI = -0.1 is -0.52 and at SI = 0.1 it is about -0.72. Total dissolved carbonate concentrations also change gradually, increasing from an initial value of 0.0156 mol/kg to 0.043 mol/kg near to equilibrium [*i.e.*, at SI(calcite) = 0.043].

There is some discrepancy between the amount of reacted $CO_2(g)$ calculated using the back-titration model (*i.e.*, 0.0055 mol/kg) and the amount of $CO_2(g)$ separated at the wellhead per kg of groundwater (0.00158 mol/kg, see Section 2.4.2.2). This apparent discrepancy may

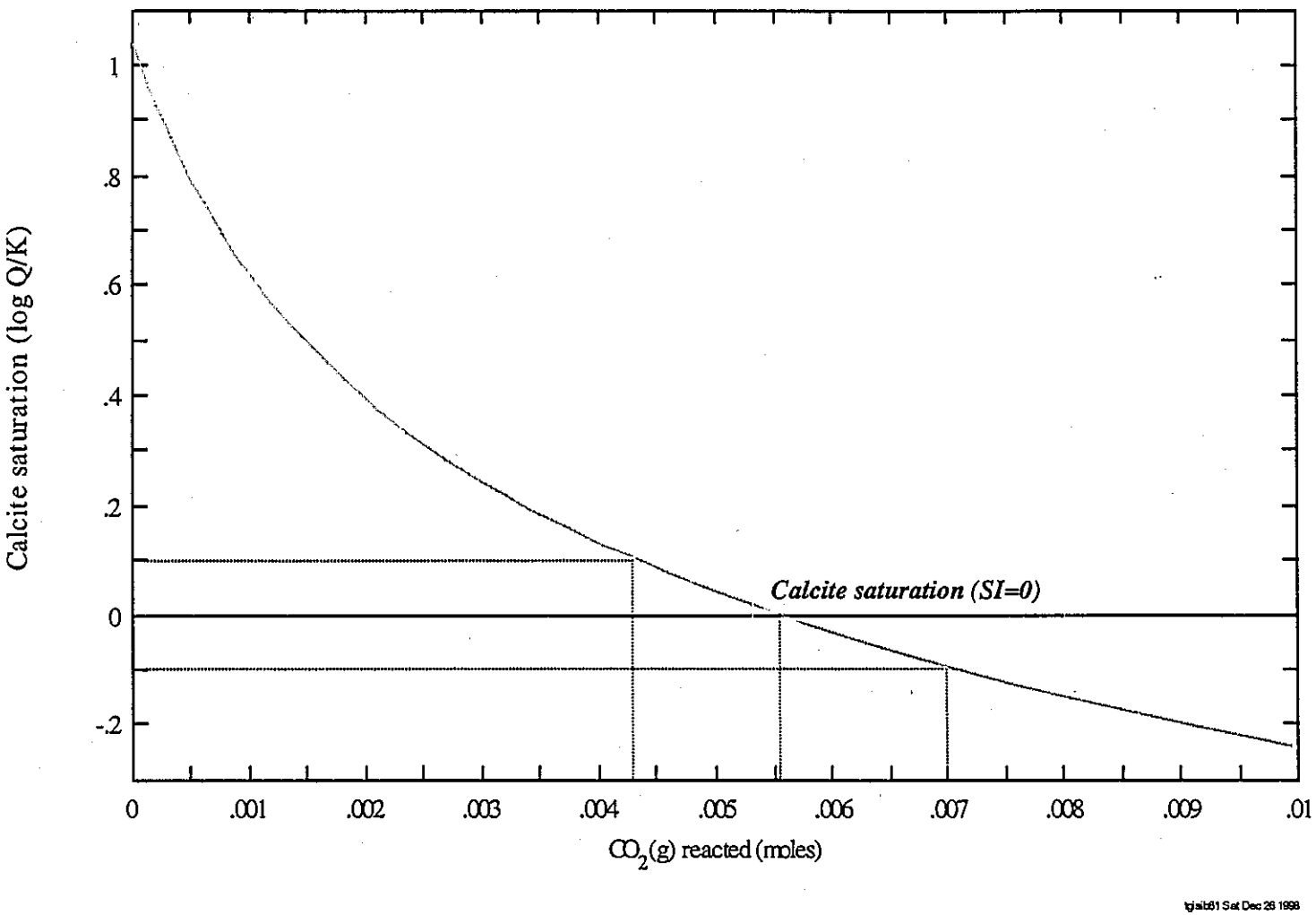

Figure 10: Variation in the calcite saturation index for the No.14 groundwater sample during $CO_2(g)$ back-titration

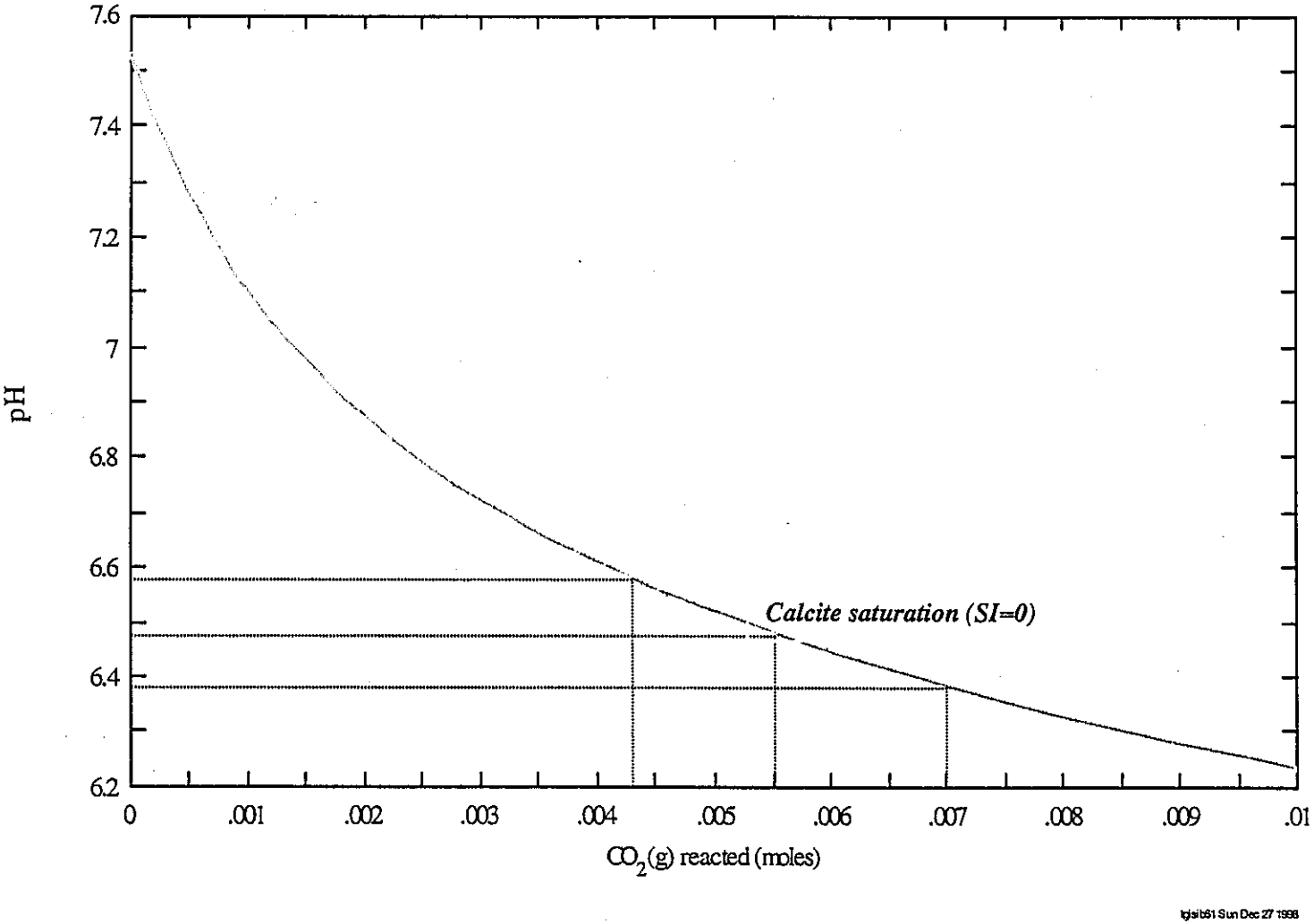

Figure 11: Variation in pH for the No.14 groundwater sample during $CO_2(g)$ back-titration

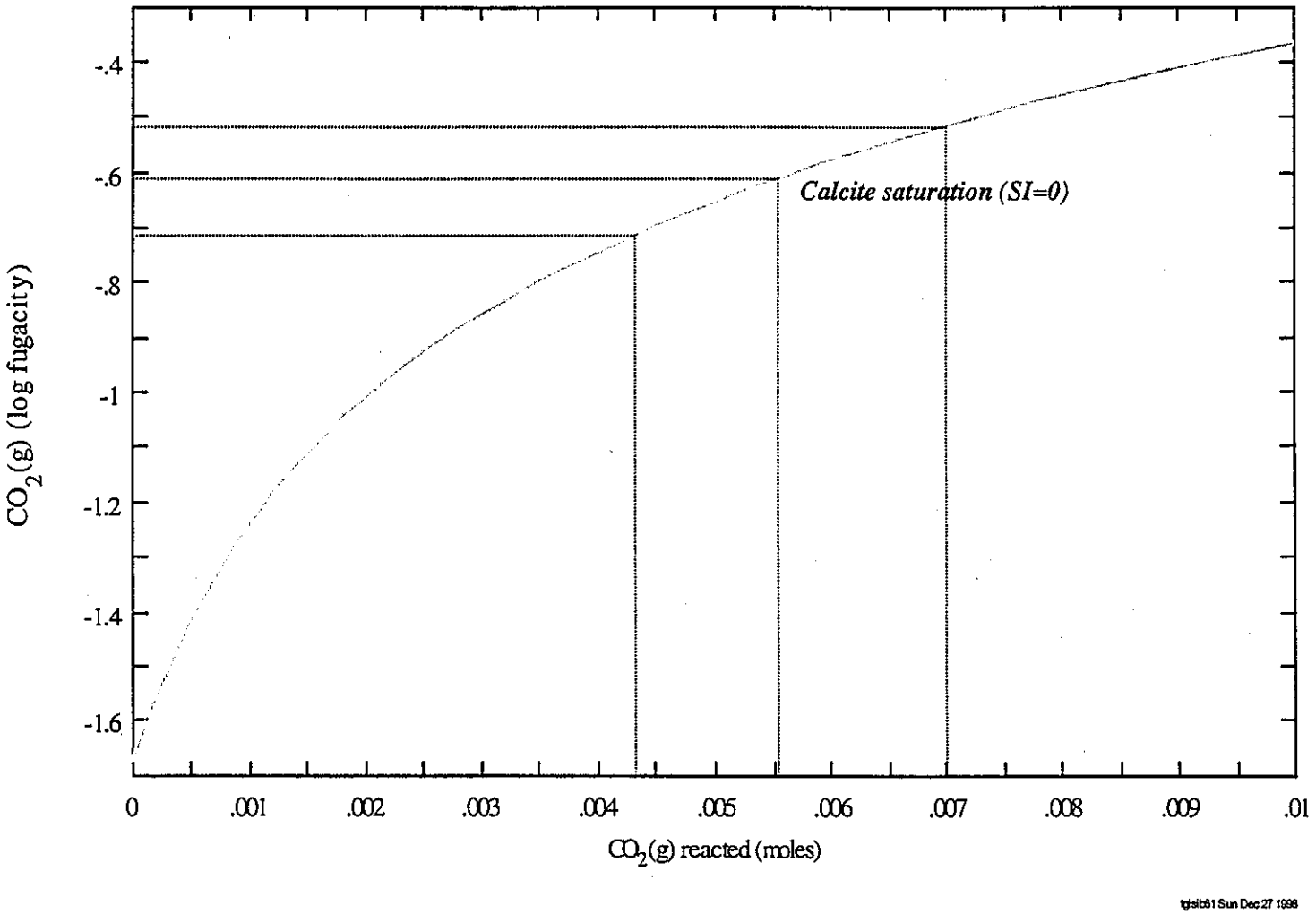

Figure 12: Variation in $logP_{CO2}$ for No.14 groundwater sample during $CO_2(g)$ back-titration

arise from uncertainties in the measurements of volumetric flow rates of liquid and gas at the wellhead, and/or to uncertainties in the composition of the gas phase. We suspect, but cannot prove at this time, that the difference between the estimates using the back-titration model and the gas-separation data are insignificant in relation to these (and perhaps other) sources of uncertainty.

2.4.3.2 Correction of Mobara Groundwater Chemistry

As noted above, the effects on pH of CO_2 degassing may be significant. To estimate the maximum likely extent of this effect for samples of Mobara-area groundwaters we assumed that the sample exhibiting the largest supersaturation with respect to calcite would have experienced the most significant amount of $CO_2(g)$ loss. The back-titration model described in Section 2.4.3.1 was therefore applied to sample No. 78 (calcite SI = 1.14, see Section 2.3). The REACT input script for this model is provided in Appendix C, and results are shown in Figure 13, assuming an in-situ temperature of 36.3℃ (Section 2.4.2.1).

The results shown in Figure 13 indicate that calculated SI (calcite) values decrease from 1.14 to 0 at equilibrium. The amount of reacted $CO_2(g)$ is about 0.0037 mole/kg at calcite equilibrium (0.003 mole/kg for SI = 0.1 and 0.0047 mole/kg for SI = -0.1:). Corresponding variations in pH (Figure 14) decrease from an initial value of 7.86 to 6.7. The pH at SI = -0.1 is 6.6 and at SI = 0.1 it is 6.8. Corresponding changes in log P_{CO2} values (Figure 15) are from -2.078 to -0.9. Log P_{CO2} at SI = -0.1 is -0.8, and at SI = 0.1 log P_{CO2} = -1.0. Total dissolved carbonate concentrations vary from an initial value of 0.0148 mol/kg to 0.0188 mol/kg near to equilibrium (*i.e.*, at SI = -0.0251).

Assuming the back-titration technique provides reasonably accurate estimates of the *in-situ* chemistry of groundwaters in the Mobara area, a preliminary assessment of mineral-water equilibria in the Otadai formation was carried out. Arthur and Wang (2000) describe a similar assessment applied to the argillaceous rocks of the London Clay formation in southern England. For example, calculated mineral stability relations in the CaO-MgO-Al_2O_3-SiO_2-H_2O system at 25℃ are shown in Figure 16, where the compositions of Mobara groundwaters, both measured and corrected, are represented by symbols. As can been seen, the measured groundwater data plot in the stability field of Mg-saponite, which conflicts with the observation that montmorillonites rather than saponites are present in the Otadai formation. The corrected data, most of which lie within the stability field of Mg-montmorillonite, may be consistent with the mineralogy of the Otadai formation, but it is

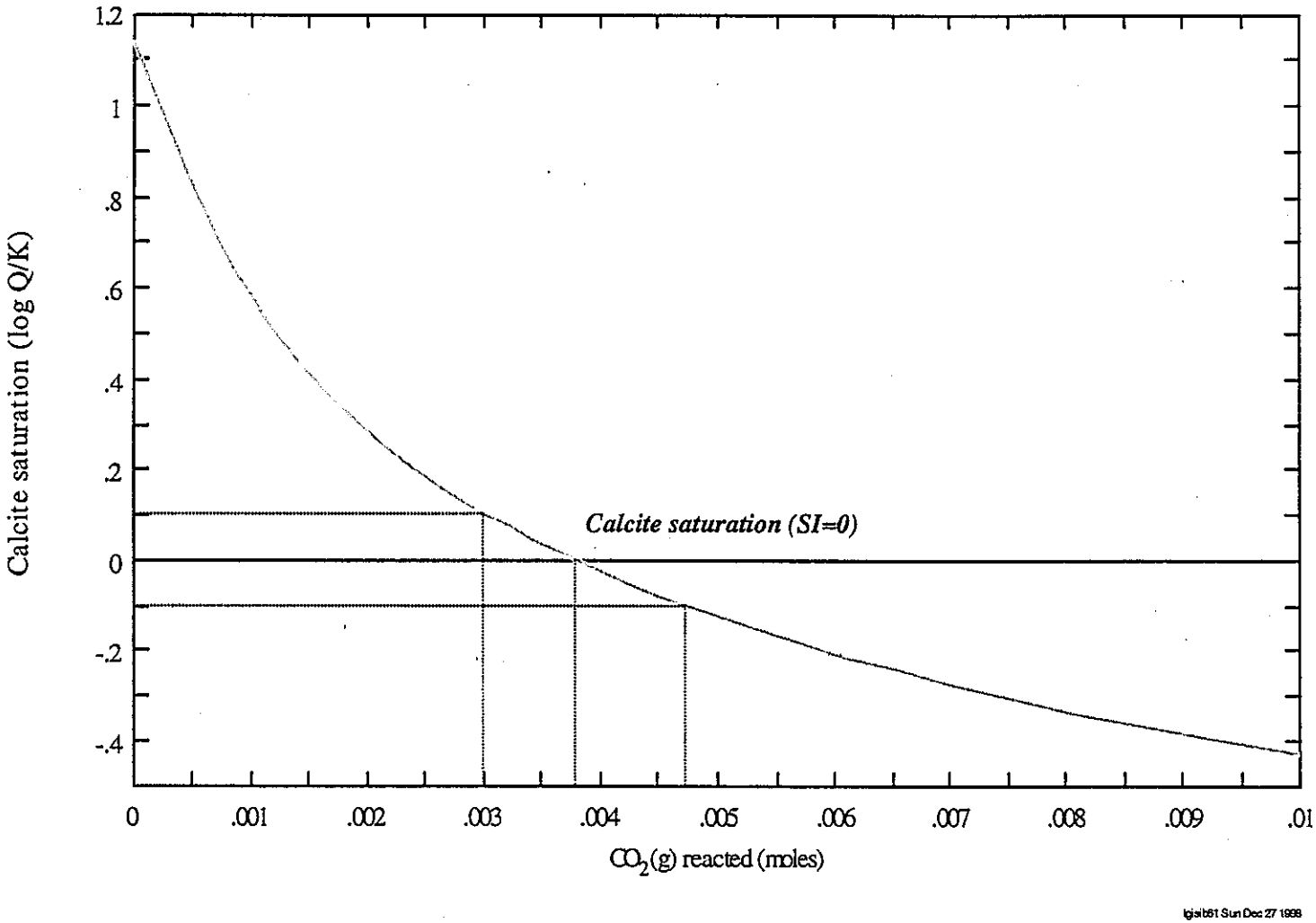

Figure 13: Variation in the calcite saturation index for No.78 groundwater sample during $CO_2(g)$ back-titration

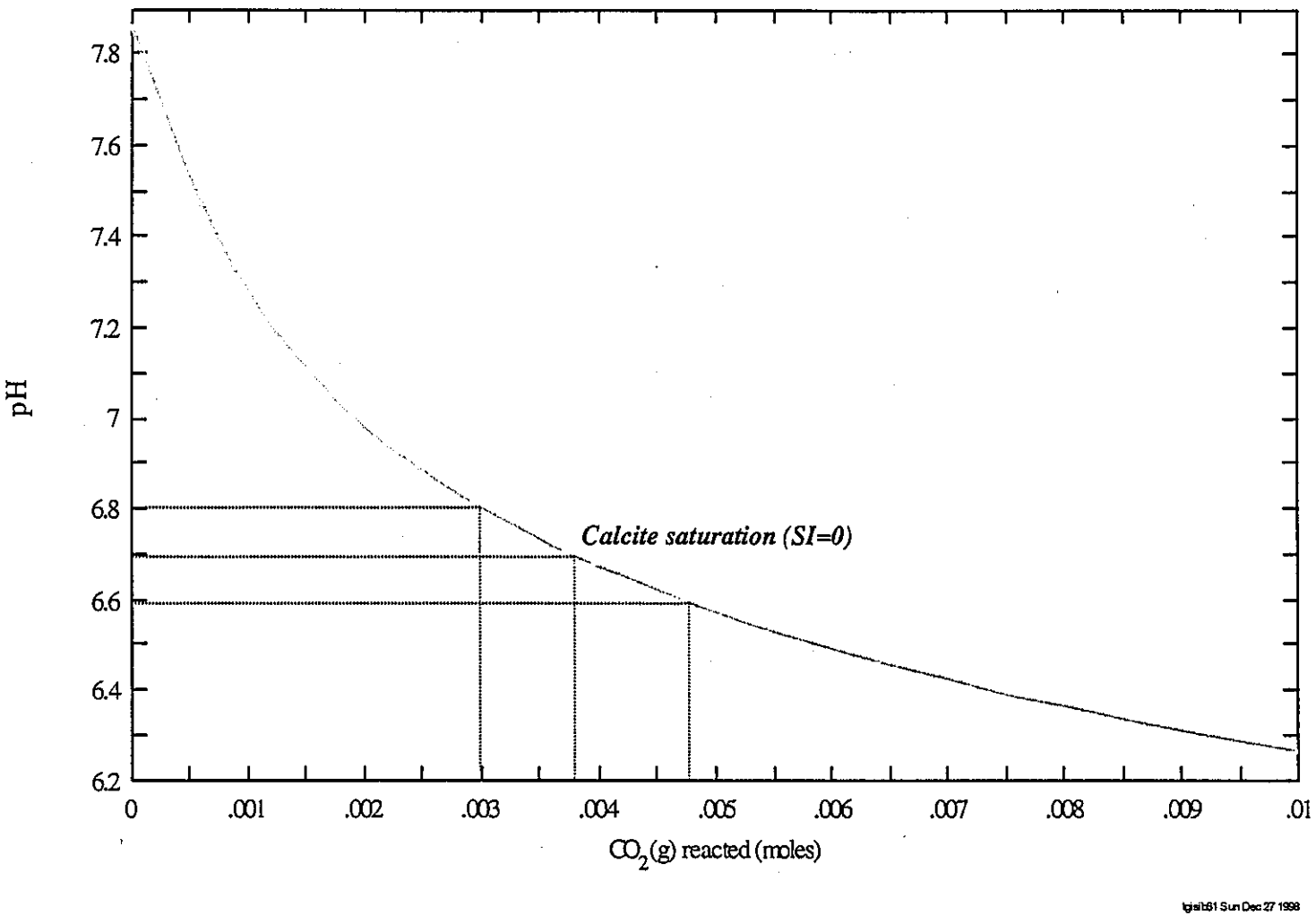

Figure 14: Variation in pH for No.78 groundwater sample during $CO_2(g)$ back-titration

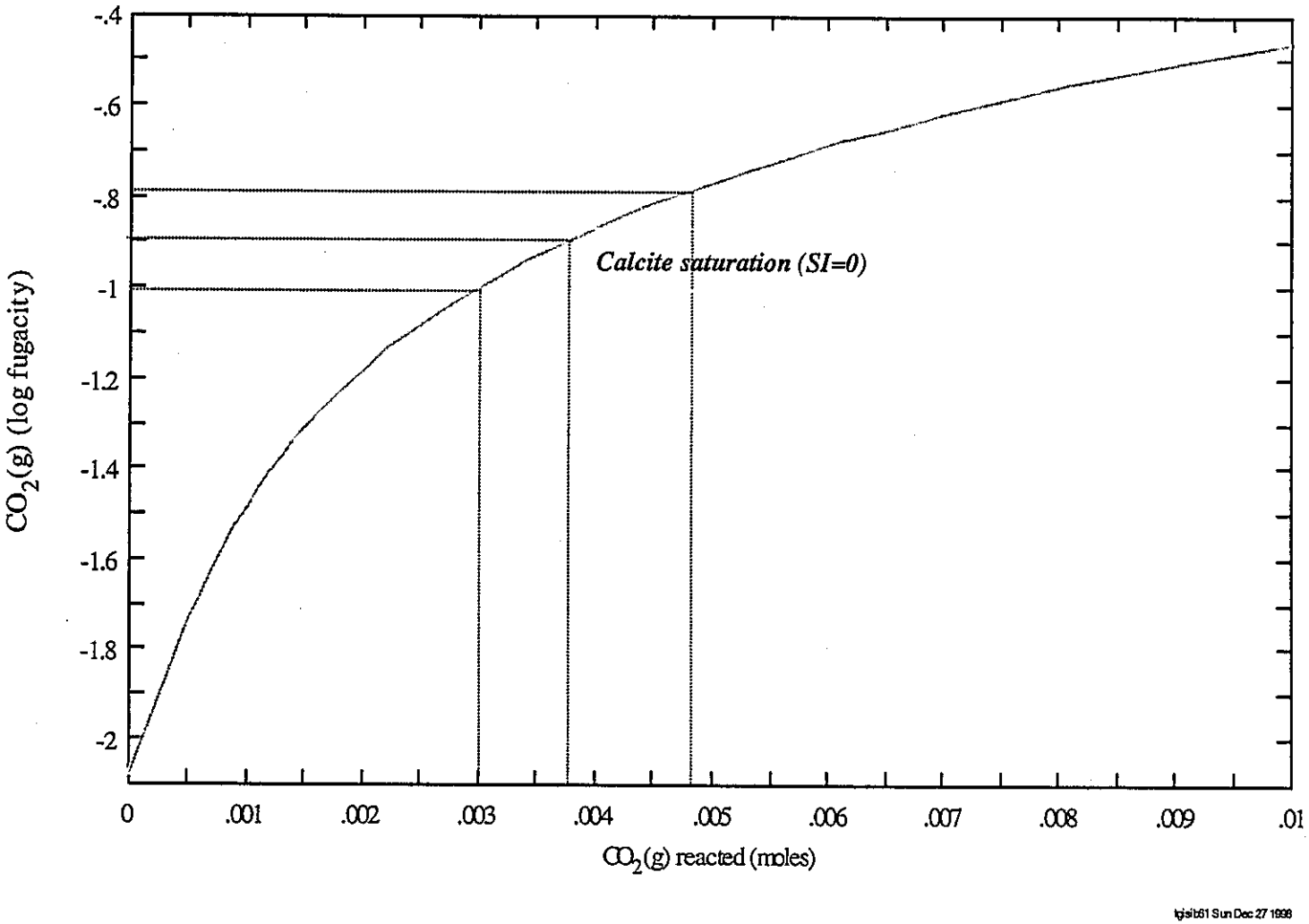

***Figure 15**: Variation in $logP_{CO2}$ for No.78 groundwater sample during $CO_2(g)$ back-titration*

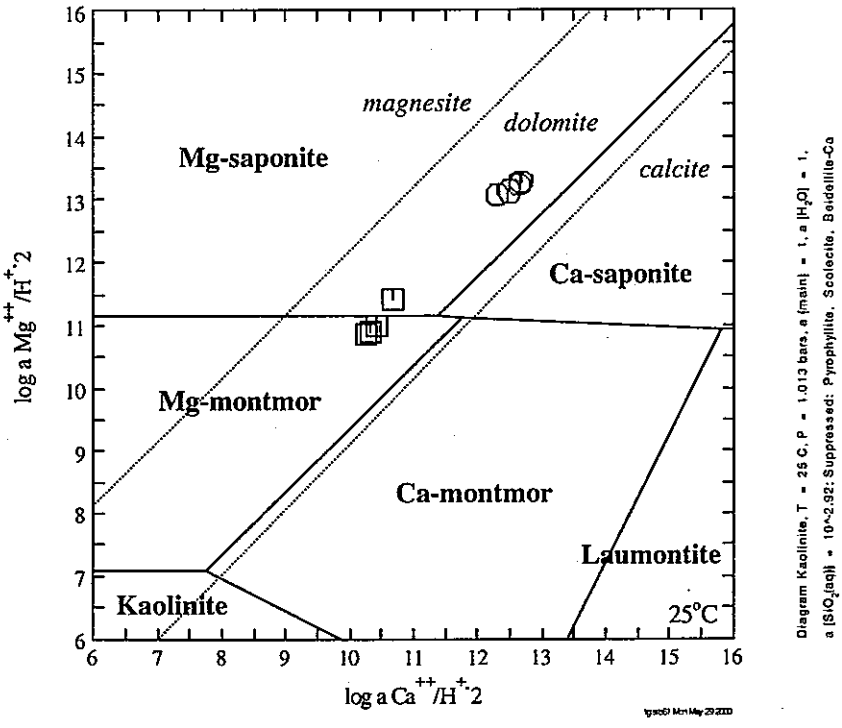

Figure 16: *Stability diagram for the CaO-MgO-Al_2O_3-SiO_2-H_2O system at 25℃, assuming log SiO_2 = -2.92 (the average SiO2 concentration for Mobara groundwaters). And also, magnesite-dolomite-calcite stability fields are overlaid on the same diagram. The circle symbols represent the composition of Mobara groundwaters based on measured pH values. On the other hand, the square symbols mean the composition of Mobara groundwaters based on corrected pH values, assuming calcite equilibrium. The thermodyanamic data for Mg-montmorillonite and Ca-montmorillonite are derived from the themodynamic database of EQ3/6 V8.R6 and added to thermo.dat database of Geochemist Workbench.*

unknown whether the montmorillonites in this formation are predominantly Mg-montmorillonite. Both the corrected and uncorrected data plot in the stability field of dolomite, but this mineral has not been observed in the Otadai formation (Kamei *et al.*, 2000). The ratios of the aqueous activities of Mg^{2+} to Ca^{2+} are greater than unity in Mobara groundwaters, indicating that calcite is unstable relative to dolomite (Stumm and Morgan, 1981). As noted earlier, the rate of dolomite precipitation is extremely slow, however. It is therefore possible that Mobara groundwaters equilibrate with calcite and are metastably supersaturated with respect to dolomite. It is also possible, however, that dolomite is present in trace amounts that cannot be detected using XRD or other analytical techniques.

Reliable Eh measurements of *in-situ* redox conditions in the Mobara area are unavailable. Kamei *et al.* (2000) evaluated redox potentials of Mobara groundwaters based on measured Eh values at the surface. It was concluded that the redox potential (Eh = -34 to -73 mV *vs.* SHE) was controlled by decomposition of organic matter to produce $CH_4(g)$. Kamei *et al.* (2000) assumed that the reaction,

$$1/4\ CH_2O + H^+ + e^- = 1/4\ CH_4(g) + 1/4\ H_2O$$

controls the redox potential of the groundwater because the calculated redox potential based on this reaction is close to Eh values measured at the surface. As noted above, however, pH values measured at surface may be unreliable due to $CO_2(g)$ degassing. If the corrected pH values are adopted for the above reaction, the calculated Eh value is about 20 mV *vs.* SHE. Such oxidizing values differ significantly from Eh values measured at the surface, which suggests that the above reaction does not control the redox potential of the Mobara-area groundwaters.

An alternative approach to that adopted by Kamei *et al.* (2000), is to assume that mineral – solution equilibria control the *in-situ* redox potentials of Mobara groundwaters. Based on the mineralogy of the Otadai formation (Section 2.2.3), reducing groundwaters should exist in this formation because pyrite and siderite coexist. Pyrite and siderite equilibrate with groundwaters relatively quickly at low temperatures, and may therefore control the redox potential these solutions.

To evaluate this possibility, equilibration of sample No. 78 groundwater with pyrite and siderite was assumed to control the *in-situ* redox potential of this solution. An Eh-pH diagram for the Fe-O-H_2O-S-CO_2 system at 36℃ (estimated *in-situ* temperature for sample

No. 78) is shown in Figure 17. The hatched circle represents the *in-situ* pH estimated the back-titration model discussed above, and *in-situ* Eh assuming equilibrium with pyrite and siderite. As can be seen, the *in-situ* Eh (about -160 mV *vs.* SHE) is significantly more reducing than the Eh measured at the surface. This suggests that the measured value may be inaccurate, possibly due to contamination with $O_2(g)$ from contact with air.

2.5 Implication of Saline-Low pH Type on Potential Deep Groundwaters

Saline groundwaters are found in many countries (*e.g.*, Sweden, Finland, Canada, Switzerland and Japan) and have been extensively investigated (*e.g.*, Grimaud *et al.*, 1990; Pitkanen *et al.*, 1996; Bradbury *et al.*, 1997). Bradbury *et al.* (1997), for example, describe a geochemical modeling study of saline porewaters in the Opalinus clay near Mt.Terri, Switzerland. Because the porosity and permeability of this formation is extremely low, it is difficult to obtain reliable *in-situ* measurements of pH and other parameters (*e.g.*, formation P_{CO2}). For this reason, Bradbury *et al.* (1997) used groundwater samples obtained from boreholes and from squeezing *in-tact* samples of the clay to approximate the *in-situ* chemistry of the clay porewaters. The experimentally determined pH values vary from 7.5 to 8, whereas the modeled pH of the porewaters is about 6. Bradbury *et al.* (1997) suggest that this discrepancy may be due to $CO_2(g)$ loss from the groundwater samples.

The present study suggests that the effects of $CO_2(g)$ degassing may also need to be considered in interpretations of the *in-situ* chemistry of deep groundwaters that are based on samples collected at the surface. As described in Section 2.4.3.2, the pH of the surface samples may be as much as 1 pH unit greater than the *in-situ* pH, which is similar to the difference observed between the measured and *in-situ* pH of Opalinus clay porewater. The corrected Mobara groundwater is inferred to be a slightly modified connate seawater that is presently reducing (Eh $\approx$ -160 mV *vs.* SHE) and slightly acidic (pH $\approx$ 6.7).

The corrected Mobara groundwater appears to be similar to the hypothetical SRLP (Saline-Reducing-Low pH) groundwater category described by JNC (Yui *et al.*, 1999). A statistical analysis of a large set of chemical analyses of groundwaters from throughout Japan did not identify the SRLP groundwater as a distinct groundwater type, possibly because of the pH of the SRLP groundwater is relatively low (Yui *et al.*, 1999). The correction method described in this report was not applied for the groundwater data set, however. Such corrections may reveal that the SRLP groundwater does exist as a distinct groundwater type in Japan, and should

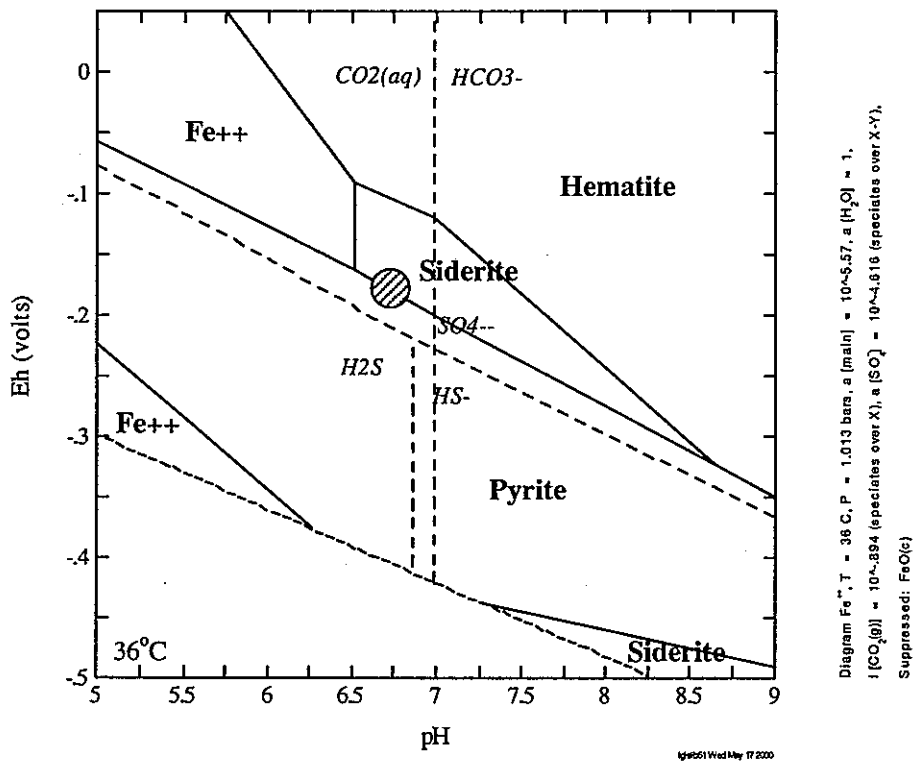

Figure 17: *Eh-pH diagram for the Fe-O-H_2O-S-CO_2 system at 36℃. Constraints used to construct the diagram are as follows; log a Fe^{2+} = -5.57, log P_{co2} = -0.894, log a SO_4^{2-} = -4.616. The hatched circle on the figure means the estimated Eh based on the corrected pH value for No.78 sample groundwater in Mobara area, assuming the groundwater equilibrated with pyrite and siderite. Interior broken lines show mosaic boundaries; labels for carbon and sulfur species were added to the diagram for clarity. Basal broken line is stability limit for water under reducing conditions at 1 atm pressure.*

therefore be included as a potential deep groundwater category in performance assessments of the Japanese disposal concept for HLW.

2.6 Summary and Recommendations

The *in-situ* geochemistry of deep groundwaters from the Mobara area, Japan are evaluated in this report based on field measurements reported by Kamei *et al.* (2000) and Sugisaki *et al.* (1962). Results suggest that the *in-situ* chemistry of Mobara groundwaters may be generally consistent with characteristics of the hypothetical SRLP-type groundwater considered in performance assessments of a deep geological repository for nuclear wastes in Japan. The failure of geostatistical methods to identify this category in a large dataset of groundwater samples from throughout Japan may be due to the fact that the samples have not been corrected for the effects of degassing during sample collection and analysis. Other results of this study are summarized as follows:

- The Mobara groundwaters appear to be slightly modified connate seawater whose age is roughly similar to the age of the Otadai formation (Neogene),
- Mobara groundwaters are Na-Cl type solutions. Elevated concentrations of K^+ and I^- in these solutions may be derived from seaweed and diatoms.
- Gas compositions in the Mobara area are dominated by $CH_4(g)$. The $CH_4(g)$ may have been generated by bacterial fermentation reactions.
- pH values measured at the surface may be unreliable indicators of the *in-situ* pH due to degassing of $CO_2(g)$ between sampling horizons in the subsurface and the wellhead. A back-titration geochemical modeling technique can be used to estimate the *in-situ* pH. This technique is based on the assumption that calcite equilibrates with Mobara groundwaters under *in-situ* conditions. The resultant, or "corrected, chemistry of Mobara-area groundwaters is more consistent with the observed mineralogy of the Otadai formation than are groundwaters whose compositions have not been corrected for the effects of degassing.
- Measured Eh values at the surface may be unreliable indicators of *in-situ* redox potentials because surface samples may be oxidized by contact with atmospheric oxygen. An analysis of mineral-equilibrium constraints on the *in-situ* Eh suggests that equilibration of Mobara groundwaters (whose pH has been corrected for the effects of degassing) with pyrite and siderite (which are present in the Otadai formation) would result in *in-situ* redox potentials that are significantly lower than Eh values measured in surface samples.

- The accuracy of groundwater data must be checked carefully considering sampling methods, measurement methods and observed mineralogy. Corrections are needed if the groundwater data are inconsistent with the chemical and physical conditions in geological formation.

To better understand the geochemical characteristics of deep saline groundwaters, the following investigations are recommended.

- A special sampling technique and apparatus should be developed to minimize the effects of degassing on groundwater compositions. The technique and apparatus may be particularly useful for future investigations that are planned by JNC at the Horonobe URL.
- Geomicrobiological and isotopic investigations are needed in future studies of deep groundwater systems. Microbes could have both a positive and negative effect on disposal of nuclear wastes. Microbes may accelerate the consumption of oxygen, for example, and may produce reducing compounds such as ferrous ion, sulfide and methane. Microbial mediation of redox reactions also may generate reducing conditions more quickly than by purely chemical reactions. Isotopic investigations are essential to obtain reliable estimates of groundwater residence times.

JNC's conceptual model for the chemical evolution of saline-type groundwaters is appropriate for sedimentary-rock environments, where reducing conditions are generated by the degradation of organic matter. Saline groundwaters are also known to exist in crystalline rocks in Japan and elsewhere (*e.g.*, Sweden, Finland, Canada *etc.*). Alternative conceptual models for the evolution of saline-type groundwaters in crystalline rocks may therefore need to be developed in the future.

3. DISCUSSION OF GROUNDWATER EVOLUTION MODELS

3.1 Executive Summary of Discussion

Field studies are being carried out by JNC to characterize the hydrogeologic and geochemical properties of three common geologic environments in Japan: granodioritic host rocks (Kamaishi area); granitic host rocks overlain by Tertiary sediments (Tono area); and intercalated mudstones and volcaniclastic sediments (Mobara area). The objectives of the field studies include *characterization* of subsurface geochemical conditions in potential repository host rocks, and *testing* of equilibrium-based geochemical models of groundwater chemistry and evolution in relation to the actual behavior of real groundwater systems.

Section 2 summarizes the results of JNC's geochemical investigation at Mobara. In contrast to similar investigations at the Kamaishi area (Sasamoto *et al.*, 1999a) and Tono area (Sasamoto *et al.*, 1999b), the Mobara study focuses primarily on characterization of subsurface geochemical conditions, with less emphasis on testing of geochemical models. The field investigation at this area is limited to collection and analysis of groundwaters from deep boreholes drilled by commercial gas companies (Kamei *et al.*, 2000), and to published analyses of groundwater compositions in samples collected from the South Kanto gas field (which includes the Mobara area).

Interpretation of subsurface geochemical conditions at Mobara is complicated because these solutions contain high concentrations of dissolved gases, and because the hydrostatic pressure at depths where the groundwater flows into wellbores (approximately 1000 meters from the surface) is relatively high (roughly 100 bars, if hydrostatic conditions are assumed). De-pressurization therefore occurs as groundwaters flow from the subsurface to the surface, which causes a portion of the dissolved gases to exsolve. Several of the dissolved gases in Mobara groundwaters are volatile weak electrolytes, and partial exsolution of these gases should therefore generate associated changes in pH, and possibly Eh (*e.g.*, Arthur and Murphy, 1989). For this reason, much of the work summarized in Section 2 is necessarily devoted to development and application of a geochemical modeling approach to evaluate the effects of degassing on the chemistry of Mobara groundwaters, and thus to characterize the chemistry of these solutions at *in-situ* pressures and temperatures in the subsurface. An

important result of the work summarized in Section 2 is that such *"corrected"* groundwater compositions imply that some deep saline groundwaters in Japan may be more similar to the hypothetical SRLP type groundwater (Yui *et al.*, 1999) than previously believed.

A discussion of the results presented in Section 2 is summarized in the following sections. Comments address primarily the rationale and approach used to correct sampled groundwater compositions for the effects of degassing. Because the main focus of Section 2 is on the effects of degassing, comments summarized in Section 3.2 are somewhat more specific than comments on similar reports for the Kamaishi and Tono areas. Recommendations based on these comments are summarized in Section 3.3.

3.2 Discussion

3.2.1 Modeling Approach

3.2.1.1 Carbonate System

The basic modeling approach, as described in Section 2.4.3, is reasonable. Adopting the calcite saturation index (± 0.1 log unit) as the end-point for back-titration of $CO_2(g)$ is realistic, and consistent with the mineralogy of the Otadai formation.

There is some discrepancy, however, between reacted $CO_2(g)$ calculated using the model (0.0055 mole/kg H_2O at calcite equilibrium, Section 2.4.3.1) versus $CO_2(g)$ estimated on the basis of Henry's law (0.00158 mole/kg H_2O, Section 2.4.2.2), as constrained by volumetric flow rates of liquid and gas phases at the wellhead, and analyses of gas compositions (Section 2.4.2.2). It would be useful to include in the text a discussion of whether such discrepancies are important. For example, could plausible variations in the flow rate of gas and liquid phases at the wellhead account for such discrepancies? Could uncertainties in the calculation of *in-situ* temperature, and associated effects on the Henry's law constant, account for the observed discrepancy?

3.2.1.2 Complementary Use of "Degassing" Models

The "back-titration" model discussed in the report is useful for predicting the pH and groundwater composition in the subsurface environment. A related and complementary

modeling approach could also be used, however, to simulate the reverse process, *i.e.*, degassing as groundwater flows to the point of sampling at the surface. For example, using the GWB input script as described in Appendix B [*i.e.*, ignoring for purposes of illustration problems in expressing input parameters in terms of mg/l (Section 2.3)], a trial-and-error approach can be used to calculate the exact amount (0.00556 mol) of $CO_2(g)$ that must be titrated into the No.14 groundwater sample in order to equilibrate the resultant solution with calcite. The reverse of this process, *i.e.*, *exsolution* of $CO_2(g)$ from the equilibrated groundwater, can be simulated using the equilibrated groundwater composition as input (Table 6), and the REACT module command:

react - 0.00556 mol $CO_2(g)$,

where the negative sign signifies that $CO_2(g)$ is to be removed from solution to simulate degassing. Results confirm that the simulated forward (back-titration) and reverse (exsolution) processes are reversible, and that the pH would rise from about 6.5 to 7.53 as 0.00556 mol $CO_2(g)$ is lost from solution (Table 7).

An advantage of evaluating such degassing models is that alternative scenarios can be evaluated to assess associated effects on the compositions of the sampled groundwaters. For example, degassing may cause carbonate minerals, and possibly other minerals, to precipitate in the wellbore or reservoir as groundwater flows toward the surface. A model to simulate this effect is summarized in Table 8, which represents the same input script as in Table 6 with modifications to allow (equilibrium) precipitation of all minerals except dolomites (*i.e.*, Dolomite, Dolomite-ord and Dolomite-dis) and magnesite. The results of this model (Table 9) suggest that degassing would raise the pH sufficiently to precipitate calcite continuously as groundwater flows to the surface. The final calculated pH [following exsolution of 0.00556 mol $CO_2(g)$], however, is significantly lower than that calculated using the similar model noted above (Table 7), in which minerals are assumed not to precipitate. This suggests that if calcite precipitation is induced in the wellbore or reservoir by $CO_2(g)$ degassing, significantly greater amounts of this gas must exsolve from solution in order to raise the pH to levels actually observed in the No.14 groundwater sample. To test this possibility further, it could be determined whether calcite is observed as "*scale*" coating wellbore surfaces, or if significant reductions in groundwater flow to the No.14 well have been observed, possibly indicating a reduction in reservoir permeability due to calcite precipitation.

Table 6: Back-titration model for No.14 groundwater sample. Titration of 0.00556 mol of CO2(g) is required to equilibrate the solution with calcite (SI=0).

```
# React script, saved Thu Apr 29 1999 by RCA
data = thermo.dat verify
temperature = 44.72
1 kg free H20
pH = 6.477
TDS = 30892
total mg/kg Ca++  = 259.5
total mg/kg Mg++  = 398.3
total mg/kg Na+   = 10860
total mg/kg K+    = 132.6
total mg/kg I-    = 111.9
total mg/kg Cl-   = 17880
total mg/kg HCO3- = 1247
total mg/kg Br-   = 104.5
precip off
react -0.00556 mol of CO2(g)
```

Table 7: Final solution composition after degassing of 0.00556 mol of CO2(g), assuming no concurrent precipitation of minerals.

```
Step #   100                 Xi = 1.0000
Temperature =  44.7 C        Pressure =  1.013 bars
pH =  7.530
Ionic strength       =   0.544462
Activity of water    =   0.983274
Solvent mass         =   1.000003 kg
Solution mass        =   1.031645 kg
Solution density     =   1.013    g/cm3
Chlorinity           =   0.520633 molal
Dissolved solids     =      30671 mg/kg sol'n
```

Reactants	moles remaining	moles reacted	grams reacted	cm3 reacted
CO2(g)	1.304e-017	-0.005560	-0.2447	

No minerals in system.

Aqueous species	molality	mg/kg sol'n	act. coef.	log act.
Cl-	0.5122	1.760e+004	0.6302	-0.4911
Na+	0.4810	1.072e+004	0.6717	-0.4907
Mg++	0.01377	324.5	0.3147	-2.3630
HCO3-	0.01153	682.2	0.6896	-2.0994
Ca++	0.004429	172.1	0.2476	-2.9601
NaCl	0.003951	223.8	1.0000	-2.4033
K+	0.003476	131.7	0.6302	-2.6595
MgCl+	0.002465	142.8	0.6717	-2.7809
NaHCO3	0.002454	199.8	1.0000	-2.6101
CaCl+	0.001980	144.9	0.6717	-2.8762
Br-	0.001350	104.5	0.6302	-3.0704
I-	0.0009099	111.9	0.6302	-3.2416
MgHCO3+	0.0005955	49.25	0.6717	-3.3980
CO2(aq)	0.0005074	21.65	1.0000	-3.2946
CaHCO3+	0.0002348	23.01	0.7121	-3.7768
CO3--	7.862e-005	4.573	0.1921	-4.8208
MgCO3	7.246e-005	5.922	1.0000	-4.1399
CaCO3	3.788e-005	3.675	1.0000	-4.4216
KCl	2.393e-005	1.730	1.0000	-4.6210
NaCO3-	1.419e-005	1.142	0.6717	-5.0209
OH-	2.019e-006	0.03328	0.6520	-5.8807
MgOH+	1.826e-006	0.07314	0.6717	-5.9112
NaOH	2.651e-007	0.01028	1.0000	-6.5765
CaOH+	5.531e-008	0.003061	0.6717	-7.4300

H+	3.695e-008	3.610e-005	0.7984	-7.5302

(only species > 1e-8 molal listed)

Mineral saturation states

	log Q/K		log Q/K
Dolomite-ord	3.6912s/sat	Aragonite	0.8780s/sat
Dolomite	3.6912s/sat	Monohydrocalcite	-0.0221
Huntite	2.8451s/sat	Nesquehonite	-1.9480
Dolomite-dis	2.2795s/sat	Brucite	-2.5510
Magnesite	1.1328s/sat	Halite	-2.6038
Calcite	1.0406s/sat	Artinite	-2.7862

(only minerals with log Q/K > -3 listed)

Gases	fugacity	log fug.
Steam	0.09131	-1.039
CO2(g)	0.02124	-1.673

		In fluid		Sorbed	
Original basis	total moles	moles	mg/kg	moles	mg/kg
Br-	0.001350	0.001350	104.5		
Ca++	0.006681	0.006681	259.6		
Cl-	0.5206	0.5206	1.789e+004		
H+	0.0003001	0.0003001	0.2932		
H2O	55.51	55.51	9.693e+005		
HCO3-	0.01553	0.01553	918.4		
I-	0.0009099	0.0009099	111.9		
K+	0.003500	0.003500	132.6		
Mg++	0.01691	0.01691	398.4		
Na+	0.4874	0.4874	1.086e+004		

		In fluid		Sorbed	
Elemental composition	total moles	moles	mg/kg	moles	mg/kg
Bromine	0.001350	0.001350	104.5		
Calcium	0.006681	0.006681	259.6		
Carbon	0.01553	0.01553	180.8		
Chlorine	0.5206	0.5206	1.789e+004		
Hydrogen	111.0	111.0	1.085e+005		
Iodine	0.0009099	0.0009099	111.9		
Magnesium	0.01691	0.01691	398.4		
Oxygen	55.55	55.55	8.616e+005		
Potassium	0.003500	0.003500	132.6		
Sodium	0.4874	0.4874	1.086e+004		

Table 8: Degassing model for No.14 groundwater sample. Input values represent "corrected" groundwater composition determined by the reaction path specified in Appendix B. Concurrent mineral precipitation is assumed to occur, except for dolomites and magnesite due to kinetic inhibition.

```
# React script, saved Thu Apr 29 1999 by RCA
data = thermo.dat verify
temperature = 44.72
1 kg free H2O
pH = 6.477
TDS = 30892
total mg/kg Ca++  = 259.5
total mg/kg Mg++  = 398.3
total mg/kg Na+   = 10860
total mg/kg K+    = 132.6
total mg/kg I-    = 111.9
total mg/kg Cl-   = 17880
total mg/kg HCO3- = 1247
total mg/kg Br-   = 104.5
precip = on
react -0.00556 mol of CO2(g)
suppress Dolomite Dolomite-dis Dolomite-ord
suppress Magnesite
```

Table 9: Final solution composition after degassing of 0.00556 mol of CO2(g), assuming concurrent calcite precipitation.

```
Step #   100                Xi = 1.0000
Temperature =  44.7 C       Pressure =  1.013 bars
pH =  6.755
Ionic strength      =  0.540872
Activity of water   =  0.983258
Solvent mass        =  1.000036 kg
Solution mass       =  1.031447 kg
Solution density    =  1.013    g/cm3
Chlorinity          =  0.520617 molal
Dissolved solids    =    30454 mg/kg sol'n
```

Reactants	moles remaining	moles reacted	grams reacted	cm3 reacted
CO2(g)	1.304e-017	-0.005560	-0.2447	
Minerals in system	**moles**	**log moles**	**grams**	**volume (cm3)**
Calcite	0.001976	-2.704	0.1978	0.07300
(total)			0.1978	0.07300
Aqueous species	**molality**	**mg/kg sol'n**	**act. coef.**	**log act.**
Cl-	0.5127	1.762e+004	0.6306	-0.4904
Na+	0.4816	1.073e+004	0.6720	-0.4900
Mg++	0.01394	328.5	0.3150	-2.3574
HCO3-	0.008770	518.8	0.6898	-2.2183
NaCl	0.003964	224.6	1.0000	-2.4019
K+	0.003475	131.7	0.6306	-2.6592
Ca++	0.003158	122.7	0.2479	-3.1063
MgCl+	0.002500	144.9	0.6720	-2.7746
CO2(aq)	0.002302	98.21	1.0000	-2.6380
NaHCO3	0.001869	152.3	1.0000	-2.7283
CaCl+	0.001415	103.7	0.6720	-3.0217
Br-	0.001349	104.5	0.6306	-3.0701
I-	0.0009098	111.9	0.6306	-3.2413
MgHCO3+	0.0004586	37.94	0.6720	-3.5112
CaHCO3+	0.0001275	12.50	0.7123	-4.0418

KCl	2.399e-005	1.734	1.0000	-4.6201
CO3--	1.000e-005	0.5820	0.1926	-5.7152
MgCO3	9.362e-006	0.7653	1.0000	-5.0286
CaCO3	3.450e-006	0.3348	1.0000	-5.4622
NaCO3-	1.812e-006	0.1458	0.6720	-5.9146
OH-	3.383e-007	0.005578	0.6523	-6.6562
MgOH+	3.101e-007	0.01242	0.6720	-6.6811
H+	2.204e-007	0.0002153	0.7984	-6.7547
NaOH	4.453e-008	0.001727	1.0000	-7.3514

(only species > 1e-8 molal listed)

Mineral saturation states

	log Q/K		log Q/K
Dolomite-ord	1.7619s/sat	Aragonite	-0.1625
Dolomite	1.7619s/sat	Huntite	-0.8617
Dolomite-dis	0.3502s/sat	Monohydrocalcite	-1.0626
Magnesite	0.2440s/sat	Halite	-2.6024
Calcite	0.0000 sat	Nesquehonite	-2.8368

(only minerals with log Q/K > -3 listed)

Gases	fugacity	log fug.
CO2(g)	0.09636	-1.016
Steam	0.09131	-1.039

		In fluid		Sorbed	
Original basis	total moles	moles	mg/kg	moles	mg/kg
Br-	0.001350	0.001350	104.5		
Ca++	0.006681	0.004704	182.8		
Cl-	0.5206	0.5206	1.790e+004		
H+	0.0003001	0.002277	2.225		
H2O	55.51	55.51	9.695e+005		
HCO3-	0.01553	0.01355	801.7		
I-	0.0009099	0.0009099	111.9		
K+	0.003500	0.003500	132.7		
Mg++	0.01691	0.01691	398.5		
Na+	0.4874	0.4874	1.086e+004		

		In fluid		Sorbed	
Elemental composition	total moles	moles	mg/kg	moles	mg/kg
Bromine	0.001350	0.001350	104.5		
Calcium	0.006681	0.004704	182.8		
Carbon	0.01553	0.01355	157.8		
Chlorine	0.5206	0.5206	1.790e+004		
Hydrogen	111.0	111.0	1.085e+005		
Iodine	0.0009099	0.0009099	111.9		
Magnesium	0.01691	0.01691	398.5		
Oxygen	55.55	55.55	8.617e+005		
Potassium	0.003500	0.003500	132.7		
Sodium	0.4874	0.4874	1.086e+004		

3.2.1.3 Redox Conditions

In order to estimate the *in-situ* redox conditions, it is assumed that pyrite-siderite equilibrium controls the Eh of Mobara groundwaters (Section 2.4.3.2). The assumed equilibrium between pyrite and siderite implies a fixed value of P_{H2S} (at a given temperature and pH), but back-titration of $H_2S(g)$, and possible effects on the *in-situ* Eh and pH of Mobara groundwaters, are not considered. There appears to be very little $H_2S(g)$ dissolved in groundwaters of the South Kanto gas field (Table 3), but a finite amount, if only a trace, must exist if these two minerals coexist at equilibrium.

A model to simulate the effects on pH and Eh of back-titrating $CO_2(g)$ and trace levels of $H_2S(g)$ into Mobara groundwater (sample No. 78) is shown in Table 10, which is based on the model specified in Appendix C. The resultant reaction path is depicted as the "S-shaped" curve on the Eh-pH diagram in Figure 18, where constraints on the activity of Fe^{2+} and fugacities of $H_2S(g)$ and $CO_2(g)$ correspond to final conditions calculated in the reaction path (Table 11). As can be seen, titration of small amounts of $H_2S(g)$ generates mildly reducing conditions that are closely consistent with equilibrium between pyrite, siderite and an aqueous solution in which the activity of Fe^{2+} corresponds to that measured in Mobara groundwaters. Moreover, the calculated reaction path is generated assuming sufficient $CO_2(g)$ is titrated (0.003778 mol) such that the final solution is also equilibrated with calcite. This suggests that both $CO_2(g)$ and $H_2S(g)$, even at trace levels, may play an important role in controlling the pH and Eh of Mobara groundwaters despite the fact that dissolved $CH_4(g)$ and other gases (Table 3) are much more abundant than $H_2S(g)$ in these solutions.

3.2.1.4 Supplementary Information Derived from Calculated Amount of Methane

The calculated amount of methane shown in Table 5 suggests that for most localities degassing must occur in the wellbores rather than in the reservoir. This is because the calculated values of P_{CH4} for all the wells (according to the procedure to calculate the partial pressure of $CH_4(g)$, described in Section 2.4.2.2), except Nos. 2, 8, 15 and 16, are less than the hydrostatic pressure at sampling depths (given in Table 2, and assuming that hydrostatic pressure increases by roughly 1 bar for each 10 m increment in sampling depth, and that the water table lies near the surface). This suggests that for wells 2, 8, 15 and 16, a gas phase must exist in the reservoir, and thus that the gas/water ratio measured at the surface includes the effects of two-phase flow in the reservoir.

Table 10: Model for back-titration of CO2(g) and a trace amount of H2S(g) into sample No.78 of Mobara groundwater.

```
# React script, saved The May 04 1999 by RCA
data = thermo.dat verify
temperature = 36.3
swap e- for O2(aq)
1 kg free H2O
pH = 7.86
Eh = -.05
total mg/l SiO2(aq) = 70
total mg/l Fe++     = .98
total mg/l Ca++     = 229
total mg/l Mg++     = 315
total mg/l Na+      = 10700
total mg/l K+       = 3020
total mg/l I-       = 131
total mg/l Cl-      = 18800
total mg/l SO4--    = 22.3
total mg/l HCO3-    = 903
total mg/l Br-      = 136
react .003778 mol of CO2(g)
react 1e-7 mol of H2S(g)
precip off
```

Table 11: Final solution composition generated by back-titration of 0.003778 mol of CO2(g) and a trace amount of H2S(g) into Mobara groundwater (Sample No.78).

```
Step #   100                    Xi = 1.0000
Temperature =  36.3 C           Pressure =  1.013 bars
pH =  6.697                     log fO2 =  -65.327
Eh =  -0.1861 volts             pe =  -3.0306
Ionic strength          =       0.582680
Activity of water       =       0.981912
Solvent mass            =       0.999996 kg
Solution mass           =       1.035612 kg
Solution density        =       1.020    g/cm3
Chlorinity              =       0.561863 molal
Dissolved solids        =          34391 mg/kg sol'n
```

Reactants	moles remaining	moles reacted	grams reacted	cm3 reacted
CO2(g)	7.549e-018	0.003778	0.1663	
H2S(g)	1.266e-022	1.000e-007	3.408e-006	

No minerals in system.

Aqueous species	molality	mg/kg sol'n	act. coef.	log act.
Cl-	0.5538	1.896e+004	0.6291	-0.4579
Na+	0.4592	1.019e+004	0.6713	-0.5111
K+	0.07672	2896.	0.6291	-1.3164
HCO3-	0.01160	683.5	0.6896	-2.0969
Mg++	0.01037	243.4	0.3158	-2.4847
CO2(aq)	0.003619	153.8	1.0000	-2.4414
Ca++	0.003591	139.0	0.2479	-3.0506
NaCl	0.003429	193.5	1.0000	-2.4649
NaHCO3	0.002729	221.3	1.0000	-2.5640
MgCl+	0.002139	123.4	0.6713	-2.8429
CaCl+	0.001938	141.3	0.6713	-2.8858
Br-	0.001702	131.3	0.6291	-2.9703
SiO2(aq)	0.001157	67.15	1.1464	-2.8772
I-	0.001032	126.5	0.6291	-3.1875
KCl	0.0005091	36.65	1.0000	-3.2932
MgHCO3+	0.0004282	35.28	0.6713	-3.5414
CaHCO3+	0.0001763	17.21	0.7124	-3.9009

SO4--	0.0001404	13.03	0.1723	-4.6163
NaSO4-	5.847e-005	6.722	0.6713	-4.4061
MgSO4	1.491e-005	1.733	1.0000	-4.8264
KSO4-	1.319e-005	1.722	0.6713	-5.0527
Fe++	1.092e-005	0.5888	0.2479	-5.5676
CO3--	1.067e-005	0.6182	0.1918	-5.6891
MgCO3	6.570e-006	0.5349	1.0000	-5.1824
NaH3SiO4	5.600e-006	0.6386	1.0000	-5.2518
FeCl+	5.447e-006	0.4802	0.6713	-5.4369
CaSO4	5.140e-006	0.6756	1.0000	-5.2891
CaCO3	3.599e-006	0.3478	1.0000	-5.4438
NaCO3-	2.283e-006	0.1830	0.6713	-5.8146
H3SiO4-	1.996e-006	0.1833	0.6713	-5.8729
FeCl2	6.465e-007	0.07913	1.0000	-6.1894
FeHCO3+	5.068e-007	0.05719	0.6713	-6.4682
H+	2.514e-007	0.0002447	0.7996	-6.6968
OH-	1.707e-007	0.002803	0.6513	-6.9540
MgOH+	1.018e-007	0.004060	0.6713	-7.1654
HS-	4.446e-008	0.001420	0.6513	-7.5382
H2S(aq)	4.220e-008	0.001389	1.0000	-7.3747
NaOH	2.157e-008	0.0008330	1.0000	-7.6662
FeCO3	1.476e-008	0.001652	1.0000	-7.8308
FeSO4	1.096e-008	0.001607	1.0000	-7.9603

(only species > 1e-8 molal listed)

Mineral saturation states

	log Q/K		log Q/K
Pyrite	2.4615s/sat	Siderite	-0.5362
Dolomite	1.5347s/sat	Monohydrocalcite	-1.0340
Dolomite-ord	1.5347s/sat	Minnesotaite	-1.1444
Quartz	0.9487s/sat	Goethite	-1.5007
Tridymite	0.7933s/sat	Huntite	-1.7389
Talc	0.7198s/sat	Pyrrhotite	-1.9540
Chalcedony	0.6873s/sat	Hematite	-1.9989
Cristobalite	0.4217s/sat	Ferrosilite	-2.0752
Dolomite-dis	0.0680s/sat	Troilite	-2.5786
Calcite	0.0000s/sat	Halite	-2.5817
Magnesite	-0.0292	Sylvite	-2.8363
Aragonite	-0.1633	Enstatite	-2.8808
Amrph^silica	-0.2593	FeO(c)	-2.9480

(only minerals with log Q/K > -3 listed)

Gases	fugacity	log fug.
CO2(g)	0.1276	-0.894
Steam	0.05820	-1.235
H2S(g)	5.560e-007	-6.255
H2(g)	8.240e-008	-7.084
CH4(g)	1.201e-008	-7.920
S2(g)	1.179e-023	-22.929
O2(g)	4.709e-066	-65.327

		In fluid		Sorbed	
Original basis	total moles	moles	mg/kg	moles	mg/kg
Br-	0.001702	0.001702	131.3		
Ca++	0.005714	0.005714	221.1		
Cl-	0.5619	0.5619	1.923e+004		
Fe++	1.755e-005	1.755e-005	0.9463		
H+	0.003589	0.003589	3.493		
H2O	55.50	55.50	9.655e+005		
HCO3-	0.01858	0.01858	1095.		
I-	0.001032	0.001032	126.5		
K+	0.07724	0.07724	2916.		
Mg++	0.01296	0.01296	304.2		
Na+	0.4654	0.4654	1.033e+004		
O2(aq)	-1.734e-007	-1.734e-007	-0.005357		
SO4--	0.0002323	0.0002323	21.54		
SiO2(aq)	0.001165	0.001165	67.59		

Elemental composition	In fluid	Sorbed

	total moles	moles	mg/kg	moles	mg/kg
Bromine	0.001702	0.001702	131.3		
Calcium	0.005714	0.005714	221.1		
Carbon	0.01858	0.01858	215.5		
Chlorine	0.5619	0.5619	1.923e+004		
Hydrogen	111.0	111.0	1.081e+005		
Iodine	0.001032	0.001032	126.5		
Iron	1.755e-005	1.755e-005	0.9463		
Magnesium	0.01296	0.01296	304.2		
Oxygen	55.56	55.56	8.584e+005		
Potassium	0.07724	0.07724	2916.		
Silicon	0.001165	0.001165	31.59		
Sodium	0.4654	0.4654	1.033e+004		
Sulfur	0.0002323	0.0002323	7.190		

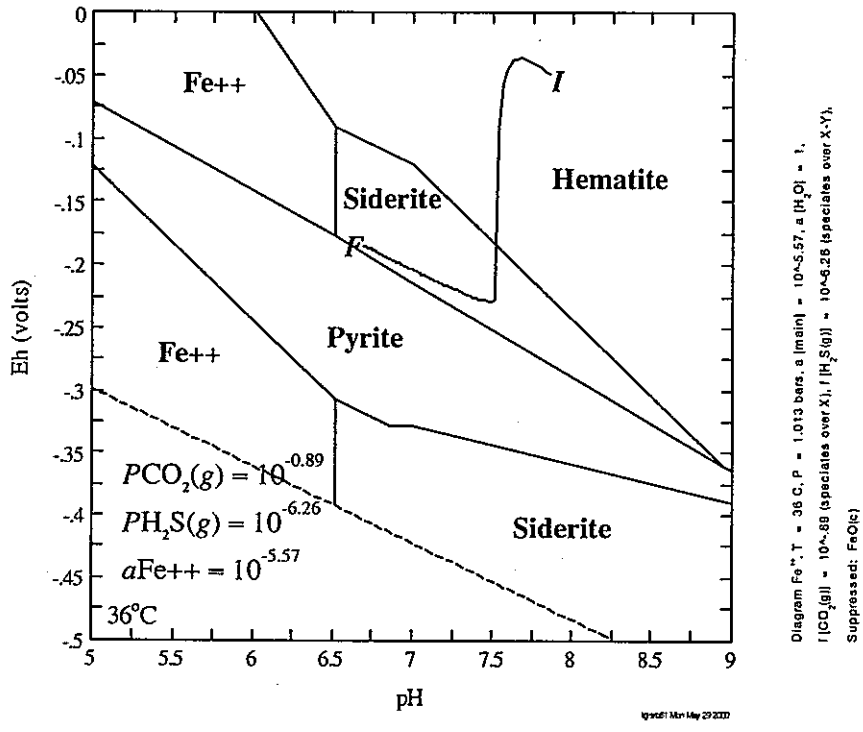

***Figure 18**: Calculated reaction path representing back-titration of $CO_2(g)$ and $H_2S(g)$ into the No.78 Mobara groundwater sample. The symbols "I" and "F" refer to initial and final compositions, respectively. Constraints used to construct the pH-Eh diagram are indicated, and are from Table 11, which specifies the final solution composition predicted by the reaction path.*

3.2.1.5 Mineralogy

The mineralogy of a sample from the Otadai formation described by Kamei *et al.* (2000) is used to constrain the back-titration models described in Section 2. In addition to calcite, pyrite and siderite, several other minerals in this formation could also be expected to equilibrate with pore fluids, including montmorillonite, illite and clinoptilolite. This raises the question whether corrected groundwater compositions, calculated using the back-titration models, are compatible with equilibrium conditions among these other minerals. To address this question, a preliminary assessment of mineral-water equilibria in the Otadai formation was carried out (Section 2.4.3.2), however. Moreover, it should be considered whether the Otadai formation is sufficiently homogeneous that a single sample of this rock can reasonably be expected to represent the mineralogy of the entire formation.

3.3 Recommendation

The concepts underlying the "back-titration" models seem to be sound. Supplementary use of "degassing models" (Section 3.2.1.2) may provide some insight into processes that could possibly occur in the wellbore and reservoir (*e.g.*, concurrent degassing and precipitation of carbonate minerals). For constraints on redox conditions, the effects of other gases, such as $H_2S(g)$, though present in trace amounts, may need to be considered.

4. CONCLUSIONS

Geochemical models for groundwater evolution in the Mobara area are tested, considering the complicated geochemical conditions such as high concentration of dissolved gases. This study focuses on characterization of the subsurface geochemical conditions in the Mobara area. Results are summarized below.

1) The geochemical characteristics of groundwaters in the Mobara area have been determined. These solutions are apparently derived from ancient seawater.

2) The accuracy of chemical analyses of deep saline groundwaters must be carefully evaluated considering sampling methods, measurement techniques and the observed mineralogy. Methods based on geochemical modeling principles (*e.g.*, the $CO_2(g)$ back-titration model discussed in this report) may be used to correct the analyses and to ensure that they are consistent with the *in-situ* chemical and physical properties of the geological formation(s) from which the samples are obtained.

3) Results of the present study considering deep saline groundwaters of the Mobara area suggest that such solutions may be more acidic than heretofore believed. Previous studies of similar systems have apparently overlooked that fact that degassing of volatile weak electrolytes [most notably $CO_2(aq)$] is possible, if not likely, and that such degassing may significantly increase the pH of groundwater samples. An important consequence of reporting analyses of saline groundwaters that have not been corrected for the effects of degassing is that the *in-situ* solutions may be considerably more acidic than indicated by the analyses, and thus possibly more similar to JNC's hypothetical SRLP groundwater than previously believed. Based on this possibility, it seems prudent to include the SRLP-type groundwater as a potential type of deep groundwater in Japan that is considered in performance assessments of the Japanese disposal concept for HLW.

4) The following issues may need to be addressed to strengthen the reliability geochemical evolution models for Mobara-area groundwaters:

· Degassing models (described in Section 3.2.1.2) may provide some insight into processes

that could possibly occur in the wellbore and reservoir (*e.g.*, concurrent degassing and precipitation of carbonate minerals).

- for constraints on redox conditions, the effects of other gases, such as $H_2S(g)$, though present in trace amounts, may needed to be considered.

5. ACKNOWLEDGEMENTS

Dr. Michael J Apted (Monitor Scientific LLC[1]) and Dr. David Savage (Quintessa Ltd[2]) contributed insightful discussions concerning JNC's groundwater evolution model. Assistance from Mr. Atsushi Neyama (Computer Software Development Corp.) and Mr. Makoto Yoshizoe (Mitsubishi Corp.) in managing the contract between JNC and MonitorScientific LLC is greatly appreciated.

[1] *Formerly QuantiSci Inc., Denver, Colorado USA*

[2] *Formerly QuantiSci Inc., Melton Mowbray UK*

6. REFERENCES

Arthur R C and Murphy W M (1989): An analysis of gas-water interactions during boiling in partially saturated tuff, *Sci. Geol. Bull.*, 42(4), pp.313-327.

Arthur R C and Wang J (2000): Claystone constraints on models of the long-term chemical evolution of buffer porewaters, In: Scientific Basis for Nuclear Waste XXXIII, R.W.Smith and D.W.Shoesmith (eds), Mat. Res. Soc. Symp., 608, Pittsburgh, PA, pp.551-556.

Bethke C M (1996): *Geochemical reaction modeling*, Oxford University Press, ISBN 0-19-509475-1.

Bradbury M H and Baeyens B (1997): Derivation of *in situ* Opalinus clay porewater compositions from experimental and geochemical modelling studies, PSI Bericht Nr.97-14 ISSN 1019-0643.

Chiba Prefecture Rsearch Institute for Environmental Pollution (1982): On the develompent of Kujyukuri gas field and its land subsidence, Project research report 5 (in Japanese).

Drever J I (1988): *The geochemistry of natural waters (second edition)*, Prentice Hall, ISBN 0-13-351396-3.

Ellis A J and McFadden I M (1972): Partial molal volumes of ions in hydrothermal solutions: *Geochim. et Cosmochim. Acta*, vol.36, pp.413-426.

Friedman L C and Erdmann D E (1982): Quality assurance practices for analyses of water and fluvial sediment (Tech. Water Resources Inc., Book 5, Chapter A6).

Grimaud D, Beaucaire C, Michard G (1990): Modellig of the evolution of ground waters in a granite system at low temperature: the Stripa ground waters, Sweden, *Applied Geochemistry*, vol.5, pp.515-525.

Ii H, Horie Y, Ishii T and Shimada J (1997): Development of an apparatus to measure groundwater qualities *in-situ* and to sample groundwater using boreholes, *Environmental Geology*, vol.32(1), pp.17-22.

Kamei G, Yusa Y and Arai T (2000): A natural analogue of nuclear waste glass in compacted bentonite, *Applied Geochemistry*, 15, pp.141-155.

Langmuir D (1997): *Aqueous eivironmental geochemistry*, Prentice Hall, ISBN 0-02-367412-1.

Matsubaya O (1985): Isotope geochemistry of geothermal water 1, *Geothermal Energy*, vol.10, No.2, pp.25-39.

Motojima K and Hirukawa T (1979): Geochemistry of some iodine-rich rocks and brines from the Mobara gas fields, 50km southeast of Tokyo, *Bull. Geol. Surv.* Japan, vol.30, pp.441-457.

Nagra (1989): Nagra bulletin, Special edition, December.

Natori H (1997): Mobara type natural gas deposits seem to be methane hydrate origin, *Chishitsu News*, No.510, pp.59-66 (in Japanese).

Nirei H (1993): Geo-environmental and einvironmenta geology, *Journal Geol. Soc.* Japan 99, pp.915-927 (in Japanese).

Nordstrom D K and Ball J W (1989): Mineral saturation states in natural waters and their sensitivity to thermodynamic and analytical errors, *Sci. Geol. Bull,* vol.42, pp.269-280, Strasbourg.

Pitkanen P, Snellman M, Vuorinen U, Leino-Forsman H (1996): Geochemical modeling study on the age and evolution of the groundwater at the Romuvaara site, Posiva 96-06, ISBN 951-6512-005-7.

PNC (1992): Research and development on geological disposal of high-level radioactive waste - First progress report -, Power and Nuclear Fuel Development Corporation., Tokai-Mura, Japan, Technical Report PNC TN1410 93-059.

Rikitake T (1992): *Handbook of earthscience (in Japanese)*, ISBN 4-7922-1332-0.

Sasamoto H, Yui M and Arthur R C (1999a): Hydrochemical investigation and status of geochemical modeling of groundwater evolution at the Kamaishi *in-situ* tests site, Japan, Japan Nuclear Cycle Development Institute., Tokai-Mura, Japan, Technical Report JNC TN8400 99-033.

Sasamoto H, Yui M and Arthur R C (1999b): Status of geochemical modeling of groundwater evolution at the Tono *in-situ* tests site, Japan Nuclear Cycle Development Institute., Tokai-Mura, Japan, Technical Report JNC TN8400 99-074.

Stumm W and Morgan J J (1981): *Aquatic chemistry (second edition)*, Willey Interscience, ISBN 0-471-09173-1.

Sugisaki R, Yoshimoto T, Kato K, Sugiura T (1962): On the relationship between the gas components and the type of the gas deposit, *Journal of Geology*, vol.69 (in Japanese).

Watanabe M, Danhara T (1996): Fission track ages of volcanic ash layers of the Kazusa Group in the Boso Peninsula, central Japan, *Journal Geol. Soc.* Japan 102, pp.545-556 (in Japanese).

Yui M, Sasamoto H and Arthur R C (1999): Groundwater evolution modeling for the second progress performance assessment (PA) report, Japan Nuclear Cycle Development Institute., Tokai-Mura, Japan, Technical Report JNC TN8400 99-030.

Appendix

Appendix A: A Method for Unit Conversion

Several units (*e.g.*, mg/l, g/l, mol/l) have been used to show the chemical compositions of groundwater data. In order to use REACT module in the GWB software, we must convert to its internal units of molality (mol/kg). To do so, the REACT module requires values for the solution's density and total dissolved solid content. According to Bethke (1996), a quick way to solve this problem is to iterate by running the REACT module, then using the calculated density and TDS as constraints on the next run, and so on until the values converge. For example, the following procedure is applied for No.1 sample in South Kanto gas field groundwaters:

[Input Script]

```
# React script, saved Tue Nov 25 1998 by H.Sasamoto
# No.1 sample in South Kanto gas field
data = thermo.dat
Temperature = 35
1 kg free H2O
pH = 7.47
total mg/l Ca++ = 169.54
total mg/l Mg++ = 156.86
total mg/l Na+ = 9706
total mg/l K+ = 226.78
total mg/l I- = 16.50
total mg/l Cl- = 16260.0
total mg/l HCO3- = 633.28
total mg/l Br- = 70.31
precip off
go
pickup density
pickup TDS
go
```

The command "precip off" means that the program does not permit mineral precipitation. The last three commands (*i.e.*, pickup density, pickup TDS and go) were repeated until density and TDS converge. To verify convergence, we checked the current density and TDS by typing "show variables" or by searching the output dataset with the commands "grep density" and "grep solids". If both values (*i.e.*, density and TDS) converge, we stopped running the program and used the output for checking the species distribution and mineral saturation.

Appendix B: React Input Script for the $CO_2(g)$ Back-Titration Model for the No.14 Groundwater Sample

```
# React script, saved Tue Nov 26 1998 by H.Sasamoto
# No.14 calcite saturation
data = thermo.dat
Temperature = 44.72
1 kg free H2O
swap CO2(g) for H+
pH = 7.53
total mg/l Ca++ = 267.73
total mg/l Mg++ = 411.01
total mg/l Na+ = 11201
total mg/l K+ = 136.85
total mg/l I- = 115.48
total mg/l Cl- = 19440.8
total mg/l HCO3- = 947.49
total mg/l Br- = 107.87
precip off
react 0.01 mol of CO2(g)
```

Appendix C: React Input Script for the $CO_2(g)$ Back-Titration Model for the No.78 Mobara Groundwater Sample

```
# React script, saved Thur Feb 19 1998 by H.Sasamoto
# Mobara No.78 groundwater sample, data from Kamei (1997)
data = thermo.dat
temperature = 36.3
swap e- for O2(aq)
swap CO2(g) for H+
1 kg free H2O
Eh = -0.05
pH = 7.86
balance on Cl-
total mg/l SiO2(aq) = 70
total mg/l Fe++ = 0.98
total mg/l Ca++ = 229
total mg/l Mg++ = 315
total mg/l Na+ = 10700
total mg/l K+ = 3020
total mg/l I- = 131
total mg/l Cl- = 18800
total mg/l SO4-- = 22.3
total mg/l HCO3- = 903
total mg/l Br- = 136
precip off
react 0.01 mol of CO2(g)
```